HERON contains contributions based mainly on research work performed in I.B.B.C. and STEVIN and related to strength of materials and structures and materials science.

Jointly edited by:

STEVIN-LABORATORY
of the Department of
Civil Engineering of the
Delft University of Technology
Delft, The Netherlands
and
I.B.B.C. INSTITUTE TNO
for Building Materials
and Building Structures,
Rijswijk (ZH), The Netherlands.

HERON vol. 20
1974
no. 2

Contents

PUNCHING SHEAR

Ir. M. Dragosavić and Ir. A. van den Beukel
(IBBC–TNO)

Preface

This research on punching shear was carried out by the Institute TNO for Building Materials and Building Structures (IBBC-TNO) with the financial support of the Netherlands Committee for Concrete Research (CUR). It was first published in Dutch as CUR Report No. 65 "Pons".

The investigations were sponsored by the CUR Committee A 18. This Committee was entrusted with the study of punching shear with a view to enabling the Netherlands delegation to the CEB (European Committee for Concrete) to take an active part in the discussion of the relevant sections of the CEB-FIP International Recommendations. The same CUR Committee was entrusted also with drawing up a proposal for incorporation into the new Netherlands code of practice for concrete, which necessitated a certain amount of further research.

In 1971 the said Committee produced an interim report on axial punching shear, based on a study of the literature and on supplementary tests. Subsequently, attention was turned to the problem of punching shear associated with eccentric load applied to columns. On the basis of test results it proved possible to derive a design formula for this loading case too. The results of the investigation of axial and eccentric punching shear for inner columns are contained in the present publication. In the mean time a start has been made with the investigation of punching shear associated with edge and corner columns.

The Committee was constituted as follows:

A. W. van IJsseldijk, Chairman
M. Dragosavić, Secretary
K. Boorsma
J. Brakel
H. van Tongeren
J. M. Lazonder, Mentor

The research was carried out by Ir. M. Dragosavić and Ir. A. van den Beukel, assisted by Ing. A. A. Kip, members of IBBC-TNO.

Thanks are due to the Netherlands Committee for Concrete Research for financing this work.

This translation into English has been prepared by Ir. C. van Amerongen, M.I.C.E.

Summary and conclusions

With a view to obtaining a better understanding of the phenomenon of shear failure at a column-to-slab connection – known as punching shear – and to establishing formulas for calculating the strength of such a connection, a study of the literature was undertaken and experimental research carried out. The results and conclusions of the investigation as a whole are described in the present report and are summarised below.

a. By punching shear is understood the failure of a slab around a column or other concentrated load, when the magnitude of the failure load is less than that corresponding to the available yield moment. This failure load is referred to as the punching resistance (ultimate punching shear force) to designate more particularly this specific type of shear failure.

b. The punching resistance of a reinforced concrete slab can, for axially applied load, be predicted by means of the following empirical formula:

$$F_{ut} = phf_{bu}$$

where:

p = $\pi(d+h)$ for round columns with diameter d
p = $2(a_1+a_2)+\pi h$ for rectangular columns with lateral dimensions a_1 and a_2, where a_1 is only a little larger than a_2
h = effective depth of the slab section
f_{bu} = average splitting tensile strength of the concrete

For the purpose of practical calculations the design value F_d of the punching resistance can be determined by substituting for f_{bu} in the above formula the design value f_b of the tensile strength:

$$F_d = phf_b$$

c. If an (external) bending moment is also acting on the column-to-slab connection, the eccentricity e (in relation to the axis of the column) due to that bending moment can be taken into account by introduction of the reduction factor α_t, so that the design value of the punching resistance is obtained from:

$$F_d = \alpha_t phf_b$$

where:

$$\alpha_t = \frac{1}{1+\frac{2e}{d+h}}$$

for round columns with diameter d.

For rectangular columns with lateral dimensions a_1 and a_2 the following value should be adopted for d in the above expression for α_t:

$$d = \frac{2}{\pi}(a_1 + a_2)$$

For the eccentricity e the ratio of the bending moment and the normal force, as obtained from the design loads C = actual loads multiplied by the appropriate load factors), should be adopted.

d. The available results of tests on specimens provided with punching shear reinforcement (i.e., reinforcement added for the purpose of increasing the punching resistance) are too few and present too wide a range of variation to justify establishing a formula which embodies also the effect of such reinforcement. The fact that punching shear reinforcement has in most cases been observed to produce some useful effect, however, suggests scope for further research.

e. Cases such as those where apertures exist in the slab in the vicinity of the column or where part of the slab adjacent to the column is absent (edge and corner columns) have not yet been sufficiently investigated to enable design rules for such cases to be established.

f. The load at which the slab fails by exhaustion of the available yield moment is determinable from conventional yield line theory. In the present report a supplementary interpretation of that theory is given for the case of combined concentrated load and concentrated bending moment (e.g., an eccentric force in a column).

Notation

A_a	cross-sectional area of one bar of the main tension reinforcement
a	width of a square column
a_1, a_2	lateral dimensions of a rectangular column ($a_1 > a_2$)
d	diameter of a round column
e	eccentricity of load on a column
F	magnitude of load on a column
F_{max}	measured maximum column load at which a specimen fails
F_{ub}	calculated maximum (column) load at which the slab fails in bending (= bending moment failure)
F_{ut}	calculated maximum (column) load at which the slab fails in shear (= punching shear failure)
F_d	design value for the shear force that can be resisted
f_e	yield point or 0,2% proof stress of the steel
f_b	design value of the tensile strength of the concrete
f_{bu}	average splitting tensile strength of the concrete $= 1 + 0{,}05 f'_{cm}$
f'_{bk}	characteristic compressive strength of the concrete
f'_b	design value of the compressive strength of the concrete
f'_{cm}	average cube strength of the concrete
f'_{bm}	average cylinder strength of the concrete
h	effective depth of the concrete section
h_t	total depth of the concrete section
l	theoretical span of a slab
l_t	total width or diameter of a slab
m_u	theoretical yield moment per unit length
n	number of observations
p	significant circumference for the punching resistance
s	centre-to-centre spacing of the main reinforcing bars
v	coefficient of variation $= \dfrac{\sqrt{\Sigma(\zeta - \zeta_m)^2/(n-1)}}{\zeta_m} 100\%$
z	internal lever arm
α_b	reduction coefficient for bending moment failure, depending on the eccentricity
α_t	reduction coefficient for punching shear failure, depending on the eccentricity
β	reduction coefficient for the external bending moment
δ	deflection of the slab at the column
δ_m	average deflection of the slab at the column
ζ	ratio of the measured and the calculated failure load $= F_{max}/\alpha_b F_{ub}$ or $F_{max}/\alpha_t F_{ut}$
ζ_m	average value of $\zeta = \Sigma\zeta/n$
$\sigma_{a.max}$	steel stress at the instant of failure

$\sigma_{b.nom}$	nominal tensile stress in the concrete
$\sigma_{b.max}$	maximum value of $\sigma_{b.nom}$
τ_{nom}	nominal shear stress in the concrete
τ_{max}	maximum value of τ_{nom}
φ	angular rotation of the axis of the column
ω_0	geometric percentage of reinforcement per unit width $= 100 A_a/hs$

Punching shear

1 Introduction

It may occur – inter alia, with flat slab floors – that a column is punched through the slab at a load which is smaller than the load deduced from the ultimate moments. This phenomenon is called punching shear.

Numerous attempts have been made to present theoretically acceptable formulas for the calculation of the punching resistance which are also in satisfactory agreement with experimental results. The value and the range of validity of the various and, to a greater or less extent, varying empirical formulas published in the literature are difficult to assess, however. On the one hand, this is due to the many factors which (may) play a part in connection with punching shear and, on the other hand, it is due to the limited number of tests on which these formulas have always had to be based.

The CUR Committee A 18, which was assigned the task of studying the problems of punching shear, set itself the objective of making recommendations for guidance in the drafting of a new Netherlands code of practice for concrete structures. To this end, a study of the available literature on the subject was first undertaken, with particular attention to the CEB Bulletin d'Information No. 57 [1], in which most of the information on punching shear investigations is assembled, and also to the punching shear tests performed in a number of countries. Furthermore, The Committee had more than forty reduced-scale model tests carried out by the IBBC-TNO (Institute TNO for Building Materials and Building Structures) with a view to obtaining a better understanding of the punching shear phenomenon and to approximately verifying the results of tests performed elsewhere.

The results of this study are summarised in the present report. From these results it appears that for axially and for centrally loaded columns – in cases where no special punching shear reinforcement has been installed in the slab – a simple formula will suffice. On comparing the results calculated by means of this formula with the test results it is found to give as good or indeed even better results than other, more elaborate formulas. For the cases where the slab does contain punching shear reinforcement and/or there are apertures in the vicinity of the column the available data are too scanty to allow a reliable opinion.

The experimental research carried out by IBBC-TNO is reported in detail in Appendix A.

2 Failure criteria

In general, a reinforced concrete slab will, as a result of increasing load, be liable to fail if one of the following two criteria is attained at one or more sections of the slab:

a. the yield point of the reinforcing steel;
b. the strength of the concrete.

In consequence of the load acting perpendicularly to the plane of the slab, bending moments and shear forces will develop at the various sections of the slab, failure usually being attributable to one of these two effects. Thus a distinction is to be drawn between bending moment failure and shear failure.

On account of the specified maximum reinforcement percentage, slabs (and beams) are so designed that as a result of the bending moment at any particular section the yield point of the main (bending moment) reinforcement will always be reached before crushing of the compression zone of the concrete occurs. The latter criterion, i.e., crushing of the concrete, is then of no practical significance with regard to bending moment failure. So there can only be *bending moment failure if the yield point of the bending moment reinforcement is the failure criterion.*

Nevertheless, failure may occur at a section before the yield point of the bending moment reinforcement is reached: it may occur in consequence of the shear force at that section. The failure is described as *shear failure if the yield point of the bending moment reinforcement does not constitute the failure criterion.* In that case failure is caused by the strength of the concrete being exceeded or by yielding of the shear reinforcement (if any).

The failure pattern envisaged in figure 1a is typical of bending moment failure; one or several wide wedge-shaped cracks develop in consequence of the point load. On the other hand, shear failure manifests itself in the formation of a wide oblique crack extending through the full depth of the slab, as indicated in figure 1b, while the bending moment reinforcement has not yet reached the yield point.

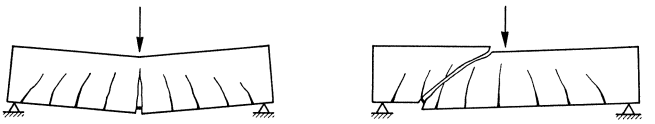

a. yielding of the steel = bending moment failure

b. failure of the concrete (before f_e is reached) = shear failure

Fig. 1. Types of failure.

Some confusion in the assessment of the failure criterion may occur if, at a certain ratio of the bending moment and the shear force during the progress of increasing the load:

- cracks first occur in accordance with figure 1a and therefore the yield point of the bending moment reinforcement has been reached;
- the yielding of the steel then continues, as a result of which the depth of the compression zone of the concrete decreases;
- finally the compression zone is no longer able to resist the combination of compressive force due to the bending moment and of shear force, so that one of the oblique cracks already present suddenly opens out through the full depth of the section.

Although the pattern that ultimately develops resembles that in figure 1b, it is nevertheless a case of bending moment failure. This is so because the slab or beam in question had, by definition, already failed at the instant when the yield point of the steel was reached.

This confusion arises also in connection with punching shear. Some engineers understand by punching shear the phenomenon that a conical portion of slab is punched out under a concentrated load, irrespective of whether this takes place before or after the yielding of the bending moment reinforcement. This is not correct, because by a *punching shear* analysis is meant solely an analysis of the slab with regard to the *shear force* occurring around a concentrated load. Since punching shear is therefore nothing but a shear failure, in the following treatment of the subject the following distinction will be drawn:

a. bending moment failure, when $\sigma_{a.max} \geqslant f_e$
b. punching shear, when $\sigma_{a.max} \leqslant f_e$

where $\sigma_{a.max}$ is the stress in the bending moment reinforcement at the instant of failure.

3 Calculation of failure load

3.1 *Analysis for bending moment with axial load on the column*

A circular slab of constant thickness, freely supported at its perimeter and carrying a point load at its centre (see figure 2a), will be considered as the basic case. The yield-line method of analysis will be used.

Bending moment failure will occur if the yield moment is reached at the radial sections. From the equation of work then follows:

$$F_{ub} \cdot \delta = \pi l \cdot m_u \cdot \frac{\delta}{\frac{1}{2}l}$$

The load at which bending moment failure occurs is therefore:

$$F_{ub} = 2\pi m_u \tag{1}$$

For a square slab (see figure 2b) the equation of work gives:

$$F_{ub} \cdot \delta = 4l \cdot m_u \cdot \frac{\delta}{\frac{1}{2}l}$$

or:

$$F_{ub} = 8m_u \tag{2}$$

The formulas given here are in principle also valid for the part of a flat-slab floor around an axially loaded column. The "free" support in figure 2 corresponds to the line of zero bending moment* at some distance from the column; the bearing reac-

* In general, the line of zero bending moment is neither a circle nor a square, but can usually be approximated by a circle, so that formula (1) will, generally speaking, provide a better approximation than formula (2) in the case of a floor slab continuous over a large number of columns.

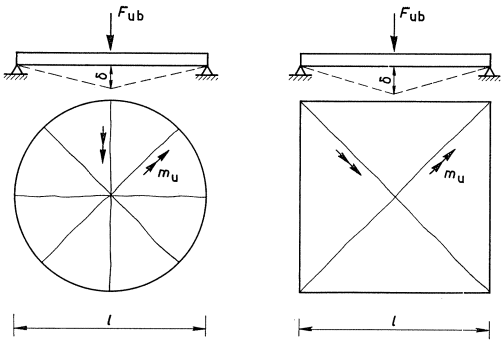

a. circular slab b. square slab

Fig. 2. Yield lines for bending moment failure.

tions thus correspond to the shear forces which occur at the line of zero bending moment.

Only if the thickness of the column is relatively large in comparison with the distance from the line of zero bending moment to the column there is any point in applying a correction expressing the ratio of these two quantities. The same can be said with regard to a slab freely supported around its perimeter and projecting some distance beyond the support, as is usually the case in tests. For the types of slab envisaged in this report the following formulas will then be applicable:

Type A. Circular slab with round column (figure 3a):

$$F_{ub} \cdot \delta = \pi l_t \cdot m_u \cdot \frac{\delta}{\frac{1}{2}l - \frac{1}{2}d}$$

or:

$$F_{ub} = 2\pi m_u \frac{l_t}{l-d} \tag{3}$$

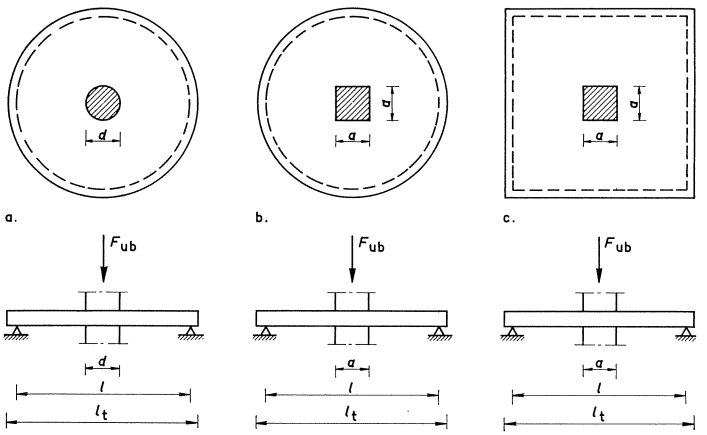

Fig. 3. Types of slab (only in the tests performed by IBBC-TNO the column was continued on the non-loaded side).

Type B. Circular slab with square column (figure 3b): The square column may be replaced by a round column of equal perimeter, so that $4a = \pi d$. From formula (3) it then follows:

$$F_{ub} = 2\pi m_u \frac{l_t}{l - \frac{4a}{\pi}} \tag{4}$$

Type C. Square slab with square column (figure 3c):

$$F_{ub} \cdot \delta = 4 l_t \cdot m_u \cdot \frac{\delta}{\frac{1}{2}l - \frac{1}{2}a}$$

or:

$$F_{ub} = 8 m_u \frac{l_t}{l - a} \tag{5}$$

Finally, in all the above formulas the yield moment m_u per unit width of the reinforced concrete section is:*

$$m_u = \frac{\omega_0}{100} f_e h z$$

or:

$$m_u = \frac{\omega_0}{100} f_e h^2 \left(1 - 0{,}56 \frac{\omega_0}{100} \frac{f_e}{f'_b}\right) \tag{6}$$

3.2 *Analysis for punching shear with axial load on the column*

The conventional assumption that punching shear failure consists in the column being "pushed through" the slab, as in figure 4a, is incorrect. In the case of a monolithic combination of column and slab this form of failure never occurs. Nor is the form of failure indicated in figure 4b ever encountered in reality either. With punching shear the ultimate fracture surface is always conical.

A more modern conception – but one which has nevertheless meanwhile also become conventional – is that the conical fracture is caused by the tensile strength being exceeded in the direction perpendicular to the conical surface at an angle of about 45° with the centre-line of the slab. This is indicated schematically in figure 4c. Such behaviour is conceivable in an uncracked slab, but in general the slab will have cracked already before the maximum load is attained, so that a considerable proportion of the conical section indicated is unable to resist tensile stresses.

After the inclined cracks have been formed (in consequence of the combination of bending moment and shear) the load is transmitted by a horizontal tensile force in

* For comparison with the test results the value adopted for f_e in formula (6) is the measured yield stress and for f'_b the average cylinder strength $f'_{bm} = 0{,}8\, f'_{cm}$. Furthermore h is the average of the two effective depths associated with the orthogonal mesh reinforcement.

the steel and the resultant of the shear force and the compressive force (due to bending moment) in the compression zone of the concrete. This is indicated in figure 4d. The triaxial state of stress in the compression zone of the concrete is complex and difficult to visualise and it may moreover depend on several variables. Hence it is not possible to express the location and magnitude of the significant concrete stresses in a formula. Besides, too little is yet known concerning the strength of concrete in a triaxial state of stress. For these reasons it has hitherto not proved possible to describe the condition(s) under which the concrete in the vicinity of the column ultimately fails and the column punches through the slab, carrying a conical piece of the latter along with it.

Also, this is why the conventional nominal shear stress τ_{nom} according to figure 4b

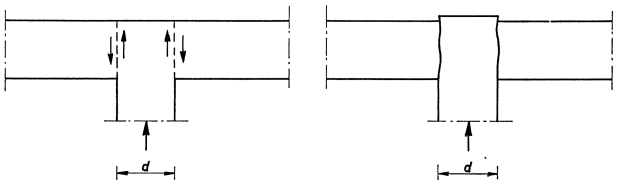

a. shearing along the column (does not occur in practice)

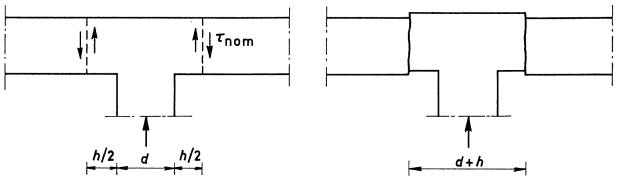

b. shearing at distance $h/2$ from the column (does not occur in practice)

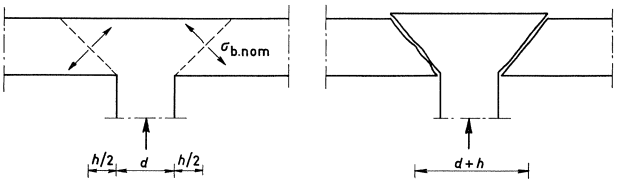

c. conical failure due to f_{bm} being exceeded (adopted as basis of formula)

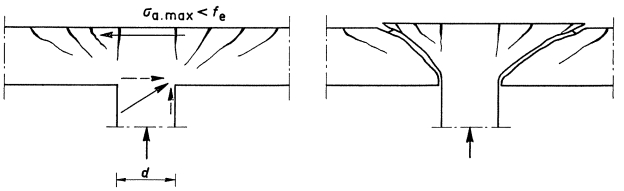

d. actual failure

Fig. 4. Forms of punching shear failure.

or the nominal tensile stress $\sigma_{b.nom}$ according to figure 4c is still adopted as the starting point in a punching shear analysis. Both stresses are conceived as acting uniformly distributed over the assumed section:

$$\tau_{nom} = \frac{F}{ph} \tag{7}$$

$$\frac{\sigma_{b.nom}}{\sqrt{2}} = \frac{F}{ph\sqrt{2}} \rightarrow \sigma_{b.nom} = \frac{F}{ph} \tag{8}$$

In both cases p is the perimeter or circumference of an area whose boundary is at a distance $\frac{1}{2}h$ from the column (see figure 5). For a round column the significant circumference is:

$$p = \pi(d+h) \tag{9}$$

For a rectangular column with sides a_1 and a_2 it is usual to conceive it as replaced by a round column whose circumference is equal to the perimeter of the rectangular column:

$$\pi d = 2(a_1 + a_2)$$

For a rectangular column the significant perimeter is then:

$$p = 2(a_1 + a_2) + \pi h \tag{10}$$

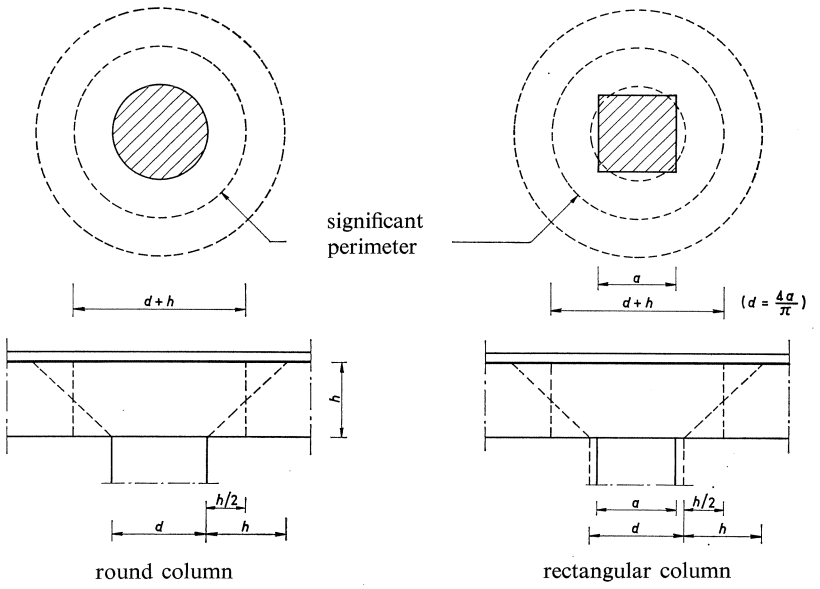

Fig. 5. Significant perimeter for punching shear analysis.

This is valid if a_1 is equal to, or not much larger than, a_2. Punching shear failure occurs when τ_{nom} or $\sigma_{b.nom}$ reaches a certain value τ_{max} or $\sigma_{b.max}$. From the formulas (7) and (8) is therefore follows for the (punching resistance) F_{ut}:

$$F_{ut} = ph\tau_{max} = ph\sigma_{b.max} \tag{11}$$

From the comparative research undertaken by the CEB (see chapter 1) it was inferred that, among the various formulas published in the literature, the best agreement with the experimental results is obtained on substituting into formula (11) the following value:

$$\tau_{max} = \frac{26\sqrt{0{,}1f'_{bk}}}{10 + \frac{l_t}{2h}} \tag{12}$$

where f'_{bk} is the characteristic compressive strength of the concrete (in N/mm^2), which is approximately equal to 0,75 f'_{cm}. This formula indicates, inter alia, that the punching resistance is dependent on the ratio of the diameter of the line of zero bending moment around the column and the thickness of the slab. However, according to the yield line theory and also according to the elastic theory, in the case of a point load this ratio ought not to affect the strength of a slab with regard to bending.* And so far as the shear force around a concentrated load is concerned, there is even less reason to suppose it to be dependent on the span of the slab: for the total shear at any particular section around the load is equal to that load itself and of course independent of the distance from the support or the line of zero bending moment.

In the CEB Recommendations only the tensile strength of the concrete is taken into account, just as in the Netherlands code of practice for concrete GBV 1962, where the above-mentioned nominal stresses are used in a somewhat modified manner.

These considerations prompted the present investigators to approach the test results with a simpler formula, which is obtained by substitution into formula (11) of:

$$\sigma_{b.max} = f_{bu} = 1 + 0{,}05f'_{cm} \tag{13}$$

where f_{bu} is the splitting tensile strength determined on cubes by the Brazilian method and f'_{cm} is the corresponding average cube compressive strength.** From the formulas (11) and (13) it now follows that:

$$F_{ut} = phf_{bu} = ph(1 + 0{,}05f'_{cm}) \tag{14}$$

* The ratio of the span to the dimensions of the area to which the concentrated load is applied is of influence, however, as is expressed in the formulas (3), (4) and (5).

** The validity of formula (13) has been experimentally demonstrated for various quality classes of gravel concrete. The reader is referred to the CUR Reports 23 and 52. The approximate formula recommended by the CEB is substantially in agreement with this.

This formula was found to provide a good approximation of the test results.

Formula (14) should not, however, be regarded as justification of the incorrect conception – associated with figure 4b or 4c – that failure due to punching shear takes place at the instant when a uniformly distributed stress (τ_{nom} or $\sigma_{b.nom}$) attains the tensile strength of the concrete at the perimeter or circumference envisaged. Formula (14) is merely an empirically established relation between the punching resistance, on the one hand, and the concrete quality, the slab thickness and the column thickness, on the other.

If the splitting tensile strength f_{bu} in formula (14) is replaced by the design value for the tensile strength of concrete f_b, the following design value is found for the shear force that can be resisted in punching shear:

$$\boxed{F_d = phf_b} \tag{15}$$

This simple formula can be recommended for the calculation of the punching resistance.

3.3 *Comparison with the test results*

3.3.1 Tests performed by IBBC-TNO

The set-up of the tests, the materials used, the manufacture of the specimens and other particulars are described in detail in Appendix A, which also gives information on cracking, the deflection measured, the form of failure and failure load measured. Figure 6 shows one of the specimens after failure, the conical shape being distinctly visible. This photograph, and others presented in Appendix A, illustrate the failure criteria discussed in chapter 2. In a very lightly reinforced slab the reinforcement

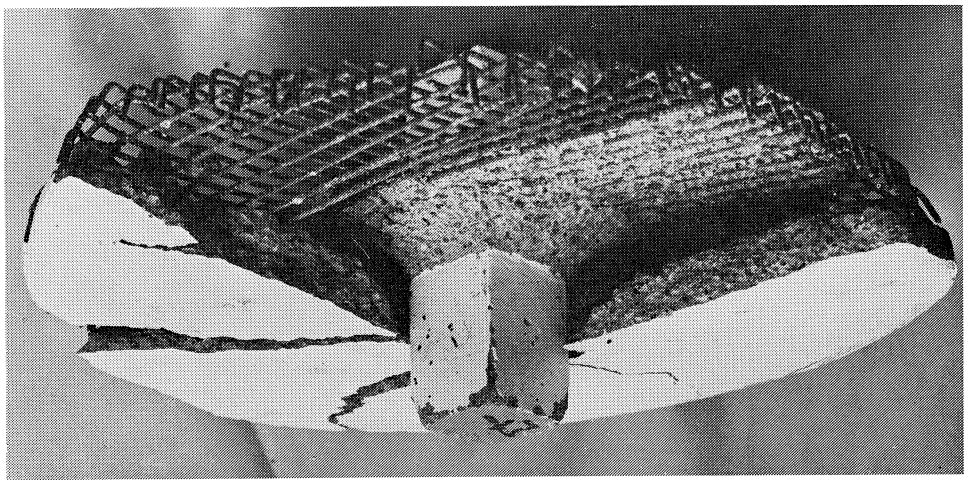

Fig. 6. Specimen II-7 after failure, viewed from below.

fractured at the radial cracks (bending moment failure). In the case of the other relatively lightly reinforced slabs a conical piece of slab was punched through, this having been preceded by yielding of the steel at the radial cracks (likewise bending moment failure). In the more heavily reinforced slabs the cone was punched through while the cracks inside and outside that cone remained narrow ($\sigma_{a.max} < f_c$; punching shear failure).

The further treatment of the subject will be confined to comparing the measured failure load F_{max} (see also column 16 in Table A1) and the calculated values for F_{ut} and F_{ub} in accordance with the formulas derived in 3.1 and 3.2 (columns 17 and 18 in Table A1).

From the foregoing it will be evident that for low percentages of reinforcement the determinative form of failure is bending moment failure, so that the failure load F_{max} will be dependent on ω_0. Above a certain percentage of reinforcement punching shear failure can be expected to occur, the magnitude of ω_0 then no longer being of significance. A preliminary general picture of the results of the tests is provided by figure 7, in which the measured values of the failure load F_{max} have been plotted against the reinforcement percentage ω_0.

In this diagram the dotted lines indicate the theoretical relation between F_{max}, on the one hand, and F_{ub} and F_{ut}, on the other hand, basing oneself on the average material properties of the test specimens. The comparison between the measured

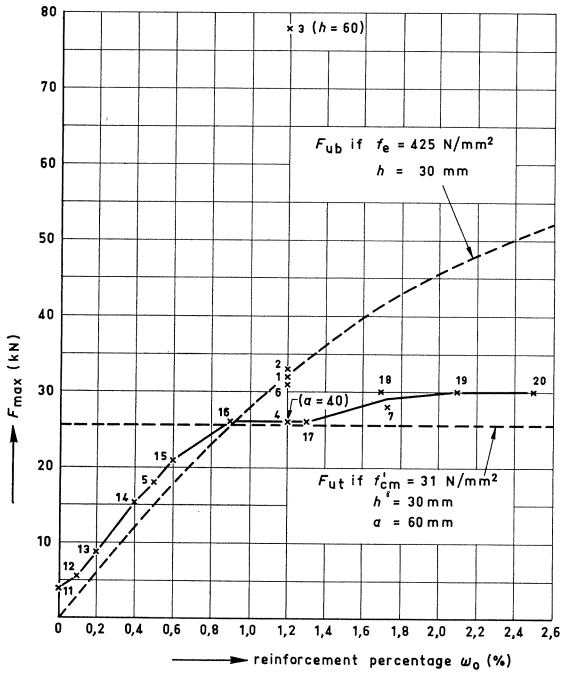

Fig. 7. Effect of reinforcement percentage ω_0 on the measured failure load F_{max}.

failure load and the calculated load is not quite correctly presented in this diagram, because the material properties of the individual specimens vary and because the specimens I-3 and I-4 have a larger slab thickness and a smaller column thickness, respectively, than the other specimens.

A better comparison is provided by figure 8, in which the ratio of the calculated values F_{ub} and F_{ut} has been adopted as the abscissae, while the ordinates represent the ratio of the measured F_{max} and the calculated punching shear force F_{ut}.* The theoretical relations $F_{max} = F_{ub}$ and $F_{max} = F_{ut}$ (in the diagram: $F_{max}/F_{ut} = F_{ub}/F_{ut}$ and $F_{max}/F_{ut} = 1{,}0$) are indicated by the solid lines in the diagram.

As expected, the test results show preference for one of the two failure criteria, depending on the percentage of bending moment reinforcement or on the ratio F_{ub}/F_{ut}. Although the test results are located somewhat above the theoretical lines, it can be asserted that the results satisfactorily follow the theoretically predicted trend.

It should be noted that in figure 8 only those specimens are represented which were axially loaded and had no punching shear reinforcement.

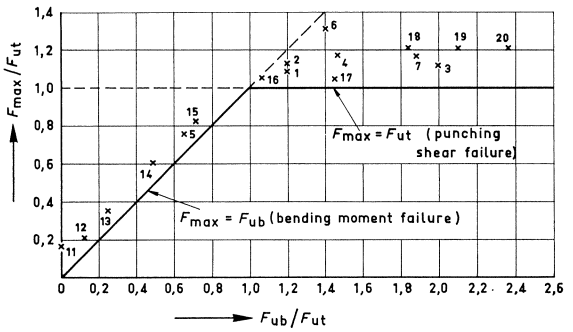

Fig. 8. Relations between F_{max}/F_{ut} and F_{ub}/F_{ut}.

3.3.2 Tests by other investigators

Besides the test results referred to in 3.3.1, additional justification of the formulas for the punching resistance F_{ut} was sought in an evaluation of results found by Elstner & Hognestad, Moe, Kinnunen & Nylander, Yitzhaki, Base and Richard. For details of those tests the CEB Bulletin d'Information No. 57 should be consulted, in which the data are presented in tables.

In that CEB publication the results are compared with the calculated values obtained with various formulas. Of the latter, the formulas (11) and (12) mentioned in this report were found to be most satisfactory.

On plotting these test results in a graph in the same manner as in figure 8, the diagram in figure 9 is obtained. It appears that the results of the total of 204 tests agree on average with theoretical lines indicated, the scatter being concentrated

* For the relevant values of F_{max}, F_{ub} and F_{ut} from the individual tests see Table A1.

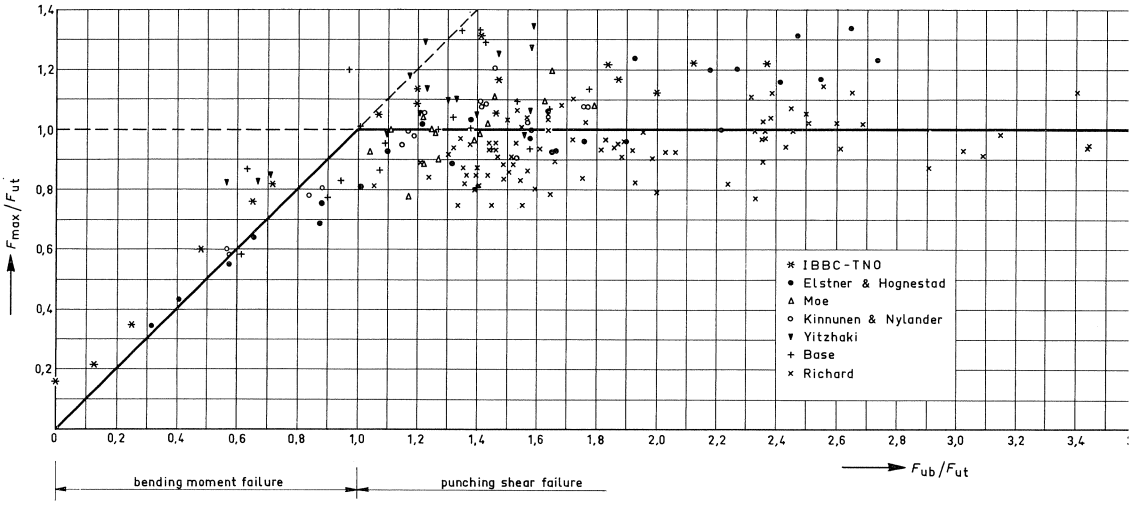

Fig. 9. Relations between F_{max}/F_{ut} and F_{ub}/F_{ut} as obtained from available test results.

Table 1. Comparison of theoretical values with test results (specimens without punching shear reinforcement)

1	2	3	4	5	6	7	8	9	10	11	12
			bending moment failure in accordance with formula (3), (4) or (5)			punching shear in accordance with formula (14)			punching shear in accordance with formula (11)+(12)		
investigators	total number of tests	type of slab (see Fig. 3)	n	ζ_m	v(%)	n	ζ_m	v(%)	n	ζ_m	v(%)
IBBC-TNO model tests	16	b	5	1,33	17,1	11	1,21	6,6	11	1,38	11,0
Elstner & Hognestad	29	c	6	0,93	11,3	23	1,05	14,0	25	1,24	15,4
Moe	17	c	0	–	–	17	0,98	11,0	14	1,16	11,1
Kinnunen & Nylander	16	a	4	0,91	7,5	12	1,04	7,7	12	1,15	13,3
Yitzhaki	16	a and b	3	1,30	11,6	13	1,14	10,6	13	1,35	9,5
Base	20	b	5	1,05	22,0	15	1,05	15,1	18	1,07	20,6
Richard (serie I)*	20	c	0	–	–	20	1,01	10,2	20	0,79	10,1
Richard (serie II)	36	c	0	–	–	36	0,96	9,2	36	0,98	17,5
Richard (series III and IV)	34	c	0	–	–	34	0,97	9,1	34	0,75	8,9
total	204		23	1,09	21,7	181	1,02	12,6	183	1,03	25,1

* In Richard's tests the slab was subjected to uniformly distributed loading. In the calculation the portion of load acting over the column itself has been deducted and the rest of the load has been assumed to act at a distance $\frac{1}{3}(l_t - a)$ from the column.

around those lines. This means that with formula (14) a satisfactory approximation is obtained for all the available test results.*

Another comparison of the calculated values and the measured values obtained in the tests is presented for the results obtained by the respective investigators in Table 1.

The number of available test results is indicated in column 2 of this table. For each specimen the failure loads F_{ub} and F_{ut} have been calculated with the aid of the formulas for the type of slab concerned. In this way it has been possible to ascertain which proportion of that number of tests must, according to the theory, have failed in bending ($F_{ub} < F_{ut}$) and which proportion must have failed in punching shear ($F_{ub} > F_{ut}$). The number of specimens for which bending was found to be the determinative condition is indicated in column 4 of the table. In column 5, for these specimens, is indicated the average ratio of the measured maximum load F_{max} and the calculated bending moment failure load F_b: $\zeta_m = \Sigma\zeta/n$, where $\zeta = F_{max}/F_{ub}$. The coefficient of variation v is given in column 6.

Similarly, the number of specimens for which punching shear was the determinative failure condition is indicated in column 7, while in column 8 the average ratio $\zeta_m = \Sigma\zeta/n$ is given, where now $\zeta = F_{max}/F_{ut}$. The coefficient of variation for this set of test specimens is given in column 9.

Finally, it appears from the table that, out of the total of 204 specimens, 23 must have failed in bending and 181 in punching shear.

The ratio of the measured to the calculated failure load for all the specimens which failed in punching shear is 1,02 on average, with a coefficient of variation of 12,6%.

If the formulas (11) and (12) are used for calculating the punching shear force F_{ut}, as has been done in the CEB publication, then the ratio F_{max}/F_{ut} is found to be 1,03 on average, with a coefficient of variation of 25,1%.

From the large difference in the magnitude of the coefficient of variation in favour of formula (14) it appears that this simple formula for calculating the punching resistance is even in better agreement with the observed values than are the formulas (11) and (12). Since moreover the quantity l_t occurs in formula (12), while the effect of this quantity on the punching resistance is open to doubt, formula (14) is to be preferred as the basis for the calculation. With due regard to the design value of the tensile strength of the concrete, it follows – as already stated in 3.2 – that:

$$\boxed{F_d = phf_b} \tag{15}$$

3.4 *Analysis for bending moment with eccentric load on the column*

In the case of eccentric column load it is an obvious choice to use the yield line theory to determine the load at which the slab succumbs to bending moment failure. In this

* The fact that the results of the tests performed by IBBC-TNO are relatively high may be attributable to membrane action and possibly to a higher quality of concrete than was ascertained from the corresponding test cubes.

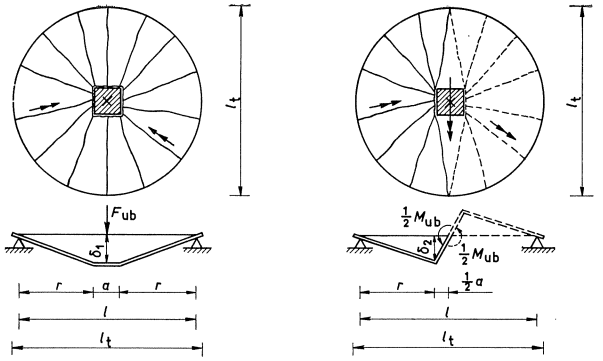

a. yield lines due to an axial load

b. yield lines due to an external moment

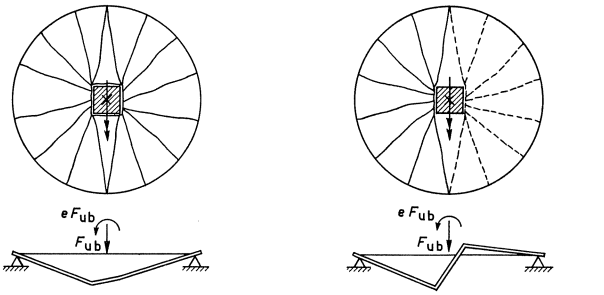

c. yield lines due to an eccentric load, if the moment is relatively small with respect to the load

d. yield lines due to an eccentric load, if the moment is relatively large with respect to the load

Fig. 10. Yield lines in the case of an arbitrary combination of axial load and bending moment.

case, however, direct application of the yield line theory is not possible, and for this reason the following approximation has been adopted.

An eccentric column load can be replaced by an axial force F and a bending moment eF.

In the case of only an axial load acting on the column the yield line pattern developed at failure would be as indicated in figure 10a. If the column exerted only a bending moment, the slab would fail with yield lines as indicated in figure 10b.

In the case where the force and the bending moment occur simultaneously, an intermediate form of behaviour is of course obtained, and it will then depend on the ratio of the force and the moment whether failure will take place according to figure 10c or figure 10d. A portion m_1 of the yield moment will in such a case be attributable to the force F_{ub}, and the other portion $m_2 = m_u - m_1$ will be caused by the bending moment $M_{ub} = eF_{ub}$.

Since the yield line patterns in figures 10a and 10b do not differ essentially (apart from the sign of the bending moment), the equation of work can be approximately established on the basis of the individual cases in figures 10a and 10b, provided that m_u is replaced by m_1 and m_2 respectively.

From figure 10a it then follows:

$$F_{ub} \cdot \delta_1 = \pi l_t \cdot m_1 \cdot \frac{\delta_1}{r}$$

or:

$$F_{ub} = m_1 \frac{\pi l_t}{r} \tag{16}$$

where:

$$r = \tfrac{1}{2}l - \tfrac{1}{2}a$$

The case represented in figure 10b can be calculated by considering one half of the slab, which is freely supported along the semicircle ($\frac{1}{2}\pi l_t$) and the straight section (l_t) and which is loaded by half the bending moment ($\frac{1}{2}M_{ub}$):

$$\tfrac{1}{2}M_{ub} \cdot \frac{\delta_2}{\frac{1}{2}a} = \tfrac{1}{2}\pi l_t \cdot m_2 \cdot \frac{\delta_2}{r} + l_t \cdot m_2 \cdot \frac{\delta_2}{\frac{1}{2}a}$$

or:

$$M_{ub} = m_2 \frac{\pi l_t}{r}\left(\frac{a}{2} + \frac{2r}{\pi}\right) \tag{17}$$

For $m_1 + m_2 = m_u$ and $M_{ub} = eF_{ub}$ the following expression for F_{ub} is obtained from the equations (16) and (17):

$$F_{ub} = m_u \frac{\pi l_t}{r} \frac{1}{1 + \dfrac{2e}{a + \dfrac{4r}{\pi}}} = m_u \frac{\pi l_t}{r} \alpha_b \tag{18}$$

For an axial load ($e = 0$, $\alpha_b = 1$) this gives the expression already derived earlier on:

$$F_{ub} = m_u \frac{\pi l_t}{r}$$

so that:

$$F_{ub(eccentric)} = \alpha_b F_{ub(axial)} \tag{19}$$

where:

$$\alpha_b = \frac{1}{1 + \dfrac{2e}{a + \dfrac{4r}{\pi}}} \tag{20}$$

The above analysis was necessary in order to ascertain which specimens may have failed in bending and should therefore be ignored in the consideration of punching shear. Because of the application of the superposition principle ($m_1 + m_2 = m_u$), which is in principle not valid at failure, the formulas (18), (19) and (20) are somewhat speculative. Although the approximation is probably on the safe side, a further study of the subject is to be recommended.

3.5 *Analysis for punching shear with eccentric load on the column*

Just as has been done in 3.2 for the case of axial column load, in the following derivation a nominal shear stress τ is considered, which is conceived as occurring in an area whose boundary is at a distance $\frac{1}{2}h$ from the column. It must again be pointed out that this conception can be usefully adopted for visualising the formula in question, but that it by no means purports to describe the actual stress distribution around the column.

The maximum vertical shear stress τ_{max} at the circular section under consideration is (figure 11):

$$\tau_{max} = \tau_{nom} + \frac{\beta M}{W} \tag{21}$$

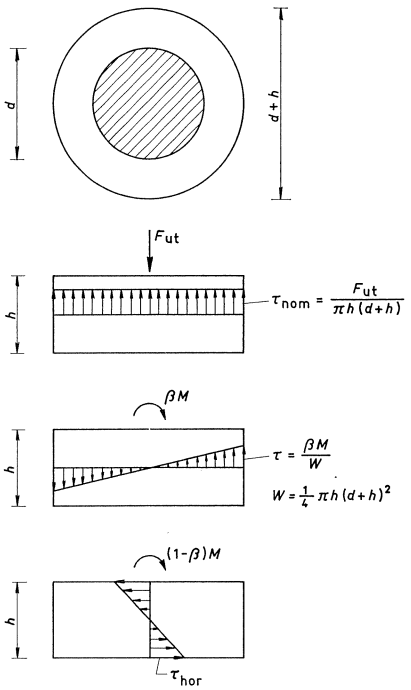

Fig. 11. Assumed shear stress distribution around an eccentrically loaded column.

where τ_{nom} is the nominal shear stress due to axial load and $\beta M/W$ is the maximum vertical shear stress due to the bending moment.

A proportion of the bending moment M is resisted by torsion of the slab, involving vertical as well as horizontal shear stresses. Since the horizontal shear stresses have no share in τ_{max}, only a proportion βM of this moment is taken into account in formula (21), while the rest of the moment, namely, $(1-\beta)M$, is ignored. W denotes the section modulus of the circumferential area with respect to the axis of the bending moment.

Substitution of $\tau_{nom} = F_{ut}/\pi h(d+h)$, $M = eF_{ut}$ and $W = \frac{1}{4}\pi h(d+h)^2$ into formula (21) gives:

$$\tau_{max} = \frac{F_{ut}}{\pi h(d+h)} \left\{ 1 + \beta \frac{4e}{d+h} \right\} \tag{22}$$

According to Mast [2] the value of β is dependent on the dimensions of the column; for a square column: $\beta = 0{,}5$.

If this value is adopted also for a round column, formula (22) becomes:

$$F_{ut} = \tau_{max} \pi h(d+h) \frac{1}{1 + \frac{2e}{d+h}} \tag{23}$$

for $e = 0$ this reduces to $F_{ut} = \tau_{max}\pi h(d+h)$, so that then:

$$\boxed{F_{ut(eccentric)} = \alpha_t F_{ut(axial)}} \tag{24}$$

where:

$$\boxed{\alpha_t = \frac{1}{1 + \frac{2e}{d+h}}} \tag{25}$$

3.6 *Comparison with the test results*

A preliminary general picture of the results of the tests performed by IBBC-TNO with eccentric column loading is provided by figure 12, which is similar in conception to figure 7. The effect of the eccentricity e, in the form of e/a, is apparent from figure 13.

The specimens intended for determining the effect of eccentricity contained bending moment reinforcement both at the top and at the bottom of the slab, in equal quantities. This reinforcement system was adopted because, according to the theory, positive as well as negative bending moments are liable to occur. For comparison, three of such specimens were subjected to axial loading only.

In 3.3.2 it has already been mentioned that for these specimens the measured failure load was relatively large (approx. 25% in excess of the calculated values: see table 1).

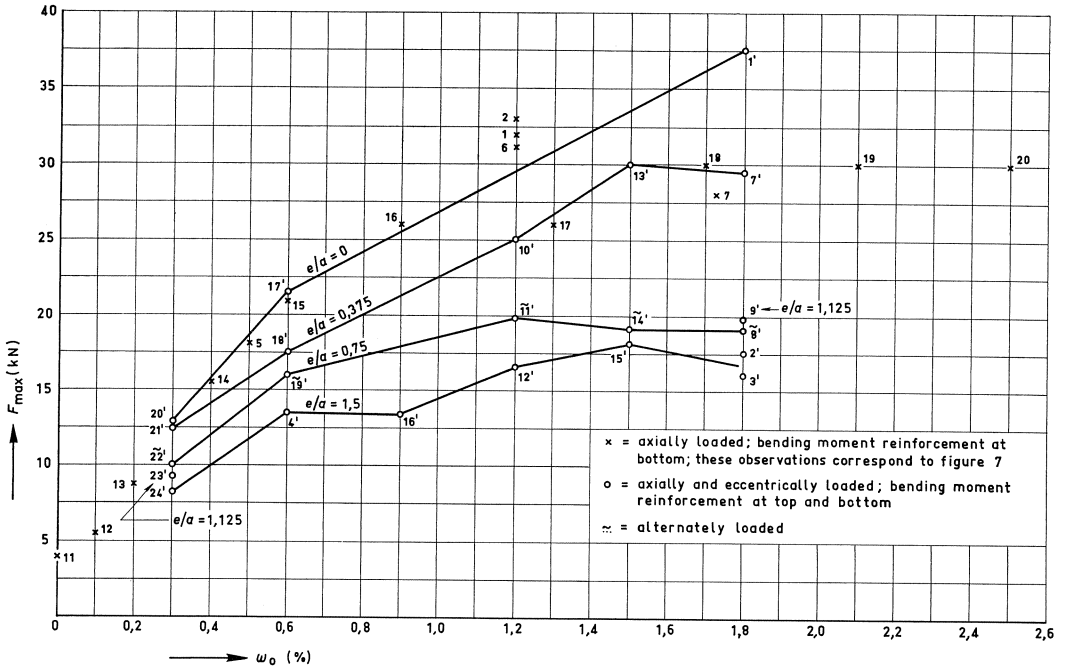

Fig. 12. Test results obtained with axially and with eccentrically loaded specimens.

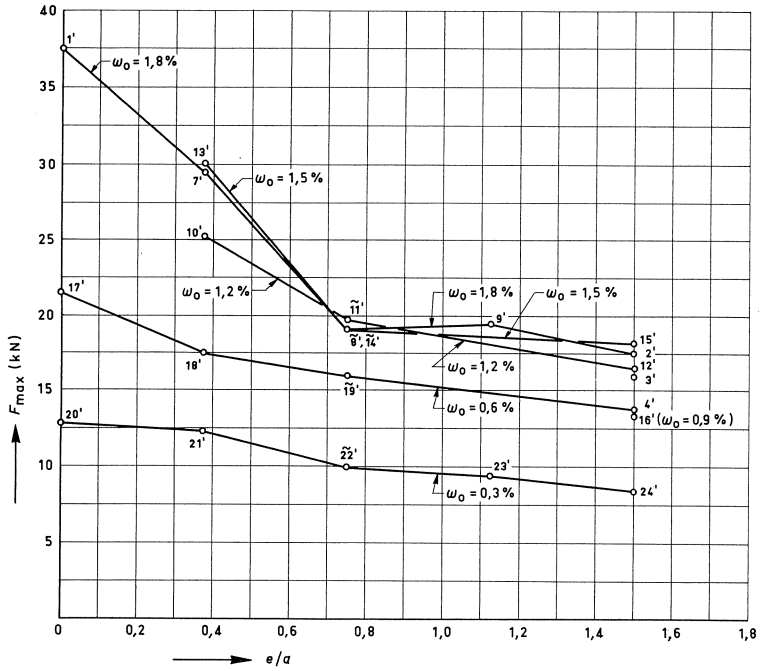

Fig. 13. Effect of eccentricity on the measured failure load.

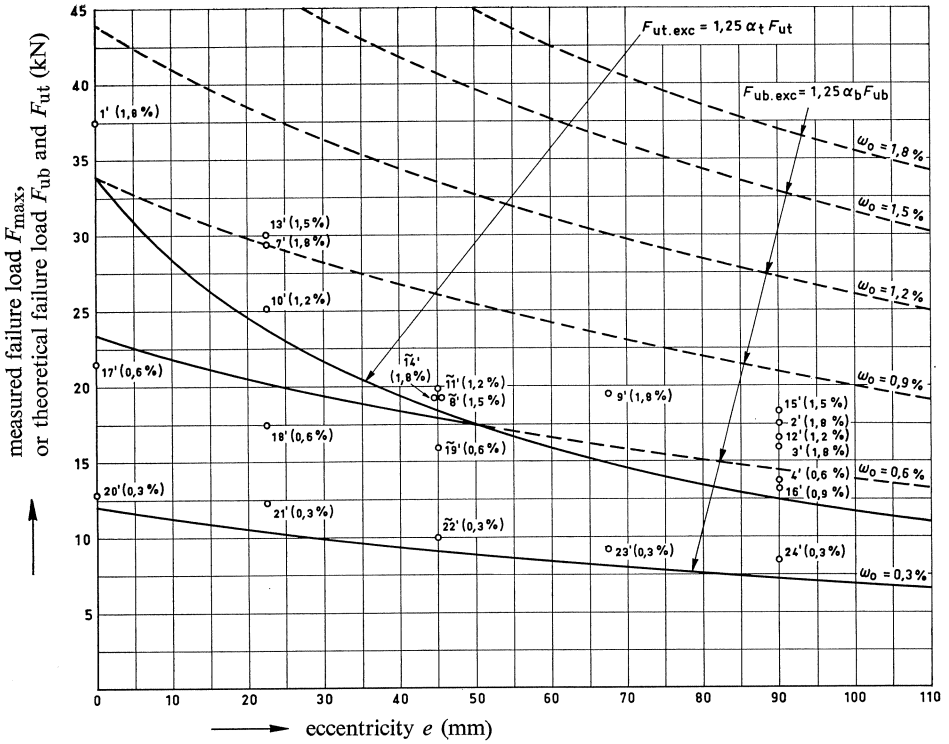

Fig. 14. Comparison of the theoretical failure load with the measured failure load.

The theoretical relation has been derived from:

$F_{ub.exc} = 1{,}25\alpha_b F_{ub}$

where: $F_{ub} = 2\pi m_u \dfrac{l_t}{l-d}$, according to formula (3)

$$m_u = \frac{\omega_0}{100} f_e h^2 \left(1 - 0{,}56 \frac{\omega_0}{100} \frac{f_e}{f_b'}\right), \text{ according to formula (6)}$$

$$\alpha_b = \frac{1}{1 + \dfrac{2e}{a + \dfrac{4r}{\pi}}}, \text{ according to formula (20)}$$

$$d = \frac{4a}{\pi}$$

$$r = \tfrac{1}{2}(l-a)$$

$F_{ut.exc} = 1{,}25\alpha_t F_{ut}$

where: $F_{ut} = \pi h(d+h) f_{bu}$, according to formulas (9), (11), (13)

$$\alpha_t = \frac{1}{1 + \dfrac{2e}{d+h}} \text{ according to formula (25)}$$

$$d = \frac{4a}{\pi}$$

For the test specimens in question:
$a = 60$ mm; $l = 425$ mm; $l_t = 475$ mm; $r = 182{,}5$ mm; $h = 29{,}5$ mm.

Therefore, in order to check the coefficients α_b and α_t, the failure loads F_{max} obtained with the specimens of series V (see table A1) have been compared with 1,25 times the corresponding theoretical values calculated with the formulas (19) and (24).

The theoretical relation between F_{ub} and F_{ut}, on the one hand, and the eccentricity e, on the other, is plotted in figure 14. Only in this diagram has been adopted: $F_{ub(exc)} = 1{,}25\alpha_b F_{ub}$ and $F_{ut(exc)} = 1{,}25\alpha_t F_{ut}$, where α_b and α_t are as expressed by the formulas (20) and (25). Comparison with the measured failure loads, likewise indicated in figure 14, shows very satisfactory agreement between the calculated and the measured values. As expected, the specimens with relatively high reinforcement percentages are found to have failed at a considerably lower value of the load than was to be expected on the basis of bending moment failure, i.e., in those cases punching shear was the governing condition as regards failure.

In the above-mentioned test specimens the eccentricity e was obtained by applying the (vertical) load at a certain distance from the axis of the column. In these tests the eccentricity was relatively small.

However, also for larger eccentricities the formula (25) gives a satisfactory relation, as witness the test results obtained by Hanson & Hanson [3], which have been plotted in figure 15, together with those of IBBC-TNO and Moe [4]. In that diagram the continuous curve indicates the theoretical relation for α_t in accordance with formula (25). The test results are found to be in excellent agreement with this curve.

It should be noted that in figure 15 only those results are included which, according to the information given in the publications concerned, represent specimens which failed in shear. The small number of specimens which underwent bending moment failure had an eccentricity $e \approx 0$, and these are not relevant to the relationship under consideration.

During the tests the force on the column was increased, while the eccentricity was always held constant. In actual practice, however, the eccentricity will usually vary.

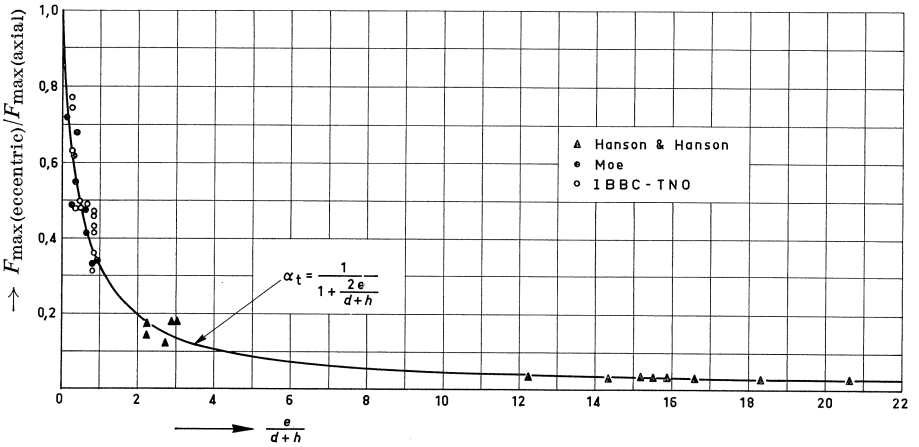

Fig. 15. Effect of eccentricity on the measured load in punching shear failure.

In that case, in the formulas (18) and (23), the eccentricity should be taken into account as the ratio of the bending moment and the normal force, both of which are obtained from the design loads.

4 Punching shear reinforcement

In CEB Bulletin No. 57, already referred to, a substantial number of tests are also reported in which the slab was provided with various types of additional reinforcement over the column in order to increase the punching resistance. As distinct from the reinforcement already provided for resisting the bending moments, this additional reinforcement is called: punching shear reinforcement.

Several investigators have tried to establish a formula in which the effect of the punching shear reinforcement on the failure load is expressed. The test results vary greatly, however, and not infrequently they are very similar to those obtained on otherwise identical specimens without punching shear reinforcement. The same general pattern emerged also in the tests described in Appendix A: specimens II-8 and II-10 attained practically the same failure load as did the specimens not reinforced for punching shear (see table A1). Specimen II-9, provided with inclined reinforcement, does show a higher punching resistance, however. Besides, in this specimen the surface of failure is found, on the underside of the slab, to begin at some distance from the column, namely, at approximately the position where the punching shear reinforcement bends up.

Tests performed with punching shear reinforcement by other investigators, in which usually (not always) a substantially higher punching resistance was found, likewise suggest that this resistance can be increased as a result of a correct choice of the shape and quantity of punching shear reinforcement. The number of tests that have so far been performed is too small, however, and their results vary too greatly to enable a well-founded design formula to be established.

Further research into the effect of punching shear reinforcement is greatly to be desired. For the time being, however, it remains advisable to attach no value to a punching shear reinforcement and, instead, to achieve improved punching resistance by increasing the thickness of the column and/or slab or by using a concrete of superior quality.

5 Other aspects

Some further aspects that also play a part in connection with punching shear will be briefly considered in this chapter.

5.1 *Alternating load*

Five specimens in the test series with eccentric column loading, as described in Appendix A, were subjected to load alternations. From the results (see, for example, figure 12, 13 and 14) it emerges that this type of loading, as compared with the results

obtained with the other specimens (under static load), did not produce results that were so much more unfavourable as to necessitate having to take account thereof. However, this conclusion is probably not validly applicable to structures which are subjected to dynamic loading conditions of long duration (e.g., machinery foundations).

5.2 *Edge and corner columns*

Although it can reasonably be supposed that for an edge column or a corner column the problem can, in principle, be tackled in the same way as in the case of the column-to-slab connections envisaged in the preceding chapters, the published information on this aspect is too scanty, so that it remains, for the present, impracticable to establish a tolerably accurate design formula for such cases.

5.3 *Local apertures around the column*

Not much is known about the effects of local apertures around the column either.

In the tests performed by Hanson & Hanson, the results of which are presented in figure 15, small apertures had been formed between column and slab along two opposite faces of the column. Such apertures, whose width was equal to one-sixth of the thickness of the column, were present in about half the specimens tested by those investigators. The bending moment reinforcement was not interrupted at these apertures, however. No difference in behaviour was found to exist in comparison with specimens in which no apertures were present. This absence of a difference can possibly be attributed to the occurrence of local stress peaks, as a result of which the concrete has an apparently higher strength.

For somewhat larger apertures it is desirable to adopt the analysis set forth in the CEB Bulletin No. 57 and in the CEB Recommendations [5]. This is briefly indicated in figure 16. With very large apertures the effect can be expected to be similar to the situation existing at an edge column, for which no analysis is as yet available. In such cases it will be necessary judiciously to apply the ordinary procedure of design to resist shear force.

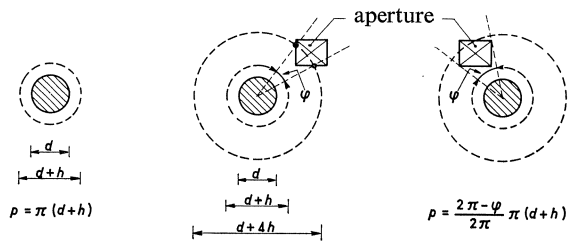

Fig. 16. Determination of the significant circumference in the case where an aperture is situated wholly or partly within a distance $2h$ from the column.

APPENDIX A

TESTS ON REDUCED-SCALE MODELS

1 General

All the investigations on punching shear in reinforced concrete slabs, as reported in the literature, have individually not made more than a modest contribution to the study of the subject. In each instance only a particular aspect of the wide-ranging set of problems involved has been investigated. The reason is that such research necessitates fairly expensive tests.

The 44 tests reported in the present publication are likewise a modest contribution. Their object is to provide approximate verification of the results obtained by other investigators (as collected in CEB Bulletin d'Information No. 57) and to obtain a better insight into the behaviour associated with failure in punching shear.

Also, with these tests, a reasonably successful attempt has been made to reduce substantially the cost of such experimental research by using scaled-down models made of micro-concrete with appropriately profiled ("deformed") reinforcement. This offers prospects of a possibly much more comprehensive research into the various aspects of punching shear, since these less expensive models make it economically possible to carry out larger numbers of tests.

The factors that affect the failure of a slab at a column are: the thickness of the column, the thickness of the slab, the quality of the concrete of the slab, the reinforcement of the slab, and the eccentricity of the load on the column. As regards the reinforcement a distinction is to be drawn between the reinforcement for resisting the bending moments and the extra reinforcement (if any) which is provided with a view to increasing the punching resistance. In the specimens tested, variations were introduced into these factors in order to ascertain their respective influence.

2 Specimens

The dimensions and other particulars of the test specimens are given in table A1 and in figure A1. To convey some idea of the scale of the models, it should be mentioned that actual structures will generally have dimensions 5 to 10 times as large as those of the specimens tested in the present research. The circular perimeter of the slab corresponds to the zero bending moment line which in an actual slab is approximately circular and is situated some distance from an (axially) loaded column. The portion of column protruding from the top of the slab suggests that in reality the column would extend over several storeys of a building; the slab therefore represents an upper floor in a multi-storey structure.

In the five specimens of series I the following were each varied once: slab thickness, column thickness, reinforcement percentage and concrete quality.

In the five specimens of series II it was investigated whether a punching shear re-

Table A1. Data and results of the model tests

1	2	3	4	5	6	7	8	9	10	11	12	13
				bending moment reinforcement					punching shear reinforcement			
series	no. of specimen	h_t (mm)	h (mm)	ω_0 (bottom) (%)	ω_0 (top) (%)	∅ (mm)	spacing of bars (mm)	f_e (N/mm²)	ω_0 (%)	∅ (mm)	spacing of bars (mm)	f_e (N/mm²)
	1	35,5	30	1,2	–	2,5	13,6	425				
	2	35,5	30	1,2	–	2,5	13,6	425				
I	3	66,0	60	1,2	–	3,0	9,8	425				
	4	35,5	30	1,2	–	2,5	13,6	425				
	5	35,5	30	0,5	–	1,6	13,4	425				
	6	35,5	30	1,2	–	2,5	13,6	425				
	7	35,5	30	1,73	–	3,0	13,6	425				
II	8	35,5	30	1,2	–	2,5	13,6	425	1,73	3,0	13,6	425
	9	35,5	30	1,2	–	2,5	13,6	425	1,73	3,0	13,6	425
	10	35,5	30	1,2	–	2,5	13,6	425	0,77	2,0	13,6	425
	11	35,5	30	–	–	–	–	–				
	12	35,5	30	0,1	–	1,2	37,7	425				
III	13	35,5	30	0,2	–	1,2	18,8	425				
	14	35,5	30	0,4	–	1,2	9,4	425				
	15	35,5	30	0,6	–	1,6	11,1	425				
	16	35,5	30	0,9	–	2,0	11,6	425				
	17	35,5	30	1,3	–	2,5	12,6	425				
IV	18	35,5	30	1,7	–	2,5	9,6	425				
	19	35,5	30	2,1	–	3,0	11,2	425				
	20	35,5	30	2,5	–	3,0	9,4	425				
	1′	35	29,5	1,8	1,8	2,5	9,1	450				
	2′	35	29,5	1,8	1,8	2,5	9,1	450				
	3′	35	29,5	1,8	1,8	2,5	9,1	450				
	4′	35	29,5	0,6	0,6	2,5	27,3	450				
	5′	35	29,5	1,8	1,8	2,5	9,1	450				
	6′	35	29,5	1,8	1,8	2,5	9,1	450				
	7′	35	29,5	1,8	1,8	2,5	9,0	450				
	8′	35	29,5	1,8	1,8	2,5	9,0	450				
	9′	35	29,5	1,8	1,8	2,5	9,0	450				
	10′	35	29,5	1,2	1,2	2,5	13,5	450				
V	11′	35	29,5	1,2	1,2	2,5	13,5	450				
	12′	35	29,5	1,2	1,2	2,5	13,5	450				
	13′	35	29,5	1,5	1,5	2,5	10,8	450				
	14′	35	29,5	1,5	1,5	2,5	10,8	450				
	15′	35	29,5	1,5	1,5	2,5	10,8	450				
	16′	35	29,5	0,9	0,9	2,5	18,0	450				
	17′	35	29,5	0,6	0,6	2,5	27,0	450				
	18′	35	29,5	0,6	0,6	2,5	27,0	450				
	19′	35	29,5	0,6	0,6	2,5	27,0	450				
	20′	35	29,5	0,3	0,3	2,5	54,0	450				
	21′	35	29,5	0,3	0,3	2,5	54,0	450				
	22′	35	29,5	0,3	0,3	2,5	54,0	450				
	23′	35	29,5	0,3	0,3	2,5	54,0	450				
	24′	35	29,5	0,3	0,3	2,5	54,0	450				

14	15	16	17	18	19	20	21	22	23	24
cube strength f'_{cm} (N/mm²)	e/a	F_{max} (kN)	F_{ut} (kN)	F_{ub} (kN)	α_t	α_b	$\zeta=\frac{F_{max}}{\alpha_t F_{ut}}$	$\zeta=\frac{F_{max}}{\alpha_b F_{ub}}$	particulars	remarks
38,4	0	32,0	29,3	35,2	1,00	1,00	1,09	(0,91)		Column 14. The compressive strength was determined on 40 mm cubes, crushed with interposition of $\frac{1}{2}$ mm thick cardboard. The stated value of f'_{cm} is 1,11 times the value obtained in the compression test. Furthermore the following were adopted: $f'_{bm}=0{,}8\,f'_{cm}$ and $f_{bu}=1+0{,}05\,f'_{cm}$
38,4	0	33,0	29,3	35,2	1,00	1,00	1,13	(0,94)		
34,1	0	78,0	69,5	138,7	1,00	1,00	1,12	(0,56)		
38,4	0	26,0	22,3	32,8	1,00	1,00	1,17	(0,79)	$a=40$ mm	
27,5	0	18,0	23,8	15,4	1,00	1,00	(0,76)	1,17		
27,7	0	31,2	23,9	33,6	1,00	1,00	1,31	(0,93)		
27,7	0	28,0	23,9	44,9	1,00	1,00	1,17	(0,62)		
29,6	0	33,6	24,9	34,0	1,00	1,00	1,35	(0,99)		
32,1	0	40,0	26,1	34,4	1,00	1,00	1,53	(1,16)		
32,1	0	32,0	20,1	34,4	1,00	1,00	1,23	(0,93)		
31,1	0	4,0	25,6	(3,7)	1,00	1,00	(0,16)	1,08		Columns 17 and 18. The value of F_{ut} has been determined from the formulas (10) and (14). The value of F_{ub} has been determined from the formulas (4) and (16). The effect of the eccentricity e has been ignored. The value of F_{ub} for specimen III-11 has been calculated with due regard to the tensile strength of the concrete (uncracked section).
31,1	0	5,5	25,6	3,2	1,00	1,00	(0,21)	1,72		
31,1	0	8,9	25,6	6,4	1,00	1,00	(0,35)	1,39		
31,1	0	15,4	25,6	12,5	1,00	1,00	(0,60)	1,23		
31,1	0	21,1	25,6	18,4	1,00	1,00	(0,82)	1,15		
29,5	0	26,0	24,8	26,5	1,00	1,00	1,05	(0,98)		
29,5	0	26,0	24,8	36,3	1,00	1,00	1,05	(0,72)		
29,5	0	30,0	24,8	45,6	1,00	1,00	1,21	(0,66)		
29,5	0	30,0	24,8	52,5	1,00	1,00	1,21	(0,57)		
29,5	0	30,0	24,8	58,8	1,00	1,00	1,21	(0,51)		
33,6	0	37,5	26,3	47,9	1,00	1,00	1,43	(0,78)		
33,6	1,500	17,5	26,3	47,9	0,37	0,62	1,80	(0,59)		
33,6	1,500	16,0	26,3	47,9	0,37	0,62	1,65	(0,54)	column rotated 45°	
33,6	1,500	13,6	26,3	18,4	0,37	0,62	1,40	(1,19)		
33,6	1,500	14,8							half slab	
33,6	1,500	8,8							quarter slab	
37,0	0,375	29,5	28,0	49,4	0,70	0,87	1,50	(0,69)		Columns 21 and 22. The parentheses indicate that the failure criterion in question is not determinative. The effect of the eccentricity (α_t or α_b) is incorporated into the value of ζ.
37,0	0,750	19,2	28,0	49,4	0,54	0,76	1,27	(0,51)	alternating load	
37,0	1,125	19,6	28,0	49,4	0,44	0,68	1,59	(0,58)		
37,0	0,375	25,2	28,0	35,2	0,70	0,87	1,29	(0,82)		
37,0	0,750	19,8	28,0	35,2	0,54	0,76	1,31	(0,74)	alternating load	
37,0	1,500	16,5	28,0	35,2	0,37	0,62	1,59	(0,76)		
37,0	0,375	30,0	28,0	42,5	0,70	0,87	1,53	(0,81)		
37,0	0,750	19,2	28,0	42,5	0,54	0,76	1,27	(0,59)	alternating load	
37,0	1,500	18,2	28,0	42,5	0,37	0,62	1,76	(0,69)		
37,4	1,500	13,4	28,2	27,2	0,37	0,62	1,28	(0,79)		For all the specimens: $a=$ 60 mm (except specimen I-4) $l=425$ mm $l_t=475$ mm
37,4	0	21,6	28,2	18,7	1,00	1,00	(0,76)	1,16		
37,4	0,375	17,5	28,2	18,7	0,70	0,87	(0,87)	1,08		
40,0	0,750	16,0	29,4	18,7	0,54	0,76	(1,01)	1,13	alternating load	
40,0	0	12,9	29,4	9,6	1,00	1,00	(0,44)	1,34		
40,0	0,375	12,4	29,4	9,6	0,79	0,87	(0,60)	1,48		
40,7	0,750	10,0	29,8	9,6	0,54	0,76	(0,62)	1,37	alternating load	
40,1	1,125	9,3	29,5	9,6	0,44	0,68	(0,72)	1,42		
40,7	1,500	8,3	29,8	9,6	0,37	0,62	(0,75)	1,39		

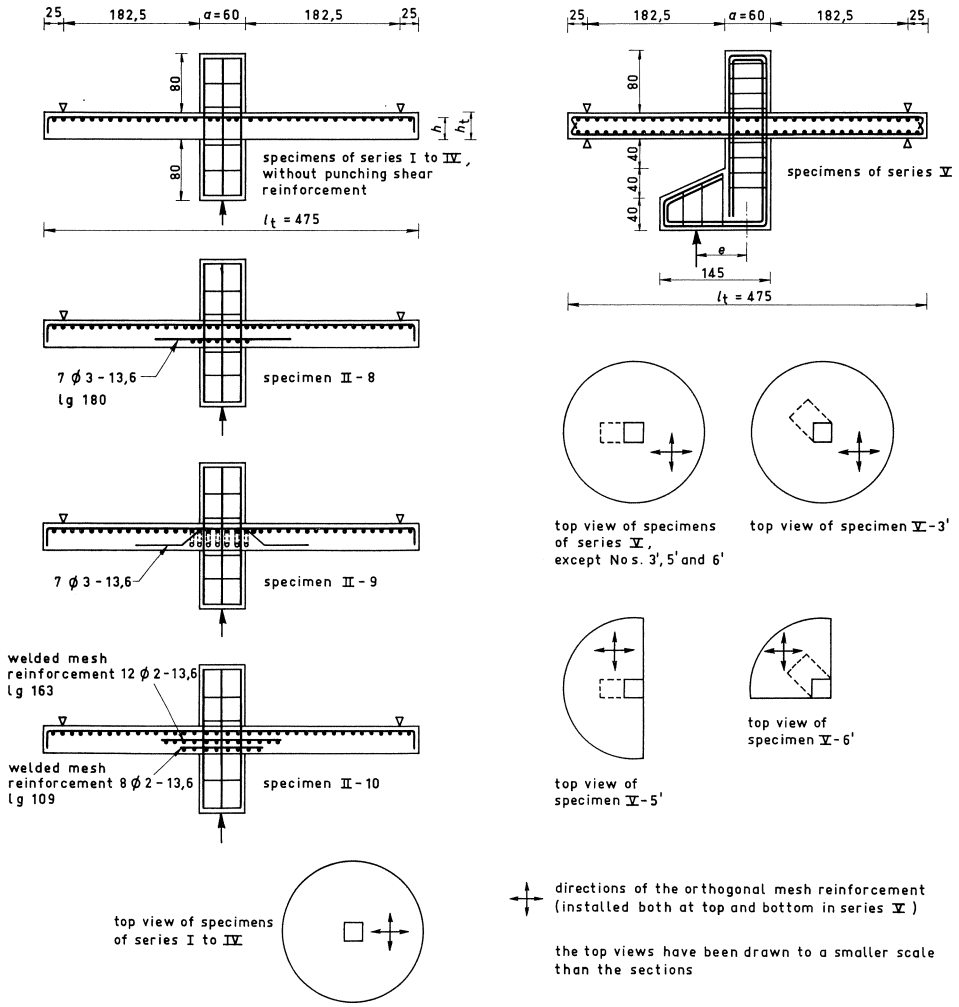

Fig. A1. Dimensions of the specimens, showing position of the reinforcement.

inforcement has an effect on the punching resistance, this being something that had not been clarified in earlier research because of the limited number of specimens tested and because of the relatively large number of variations adopted in the punching shear reinforcement under investigation.

In the ten specimens of series III and IV the percentage of bending reinforcement ω_0 was varied between 0 and 2,5% in order to determine whether bending moment failure or punching shear failure constituted the significant failure criterion at various reinforcement percentages.

In the 24 specimens of series V, apart from variation of the quantity of bending moment reinforcement, the eccentricity e of the column load was also varied between 0 and 90 mm ($e/a = 1{,}5$). At a certain eccentricity it could occur that positive as well

as negative bending moments arise in the slab; for this reason bending moment reinforcement, in equal quantities, was installed both at the top and at the bottom of the slab in all the specimens of series V. This series also included one specimen comprising a slab of semicircular shape and one specimen with a quarter-circular slab.

3 Reinforcement of the specimens

In choosing the reinforcement it was presupposed that in an actual (full-size) structure the steel employed would be ribbed FeB 400 HW, with diameters ranging from 10 to 30 mm, depending on the total quantity of steel to be installed in the vicinity of a column.

In the test specimens the reinforcing bars employed had diameters of 1,2, 1,6, 2,0, 2,5 and 3,0 mm, consisting of steel conforming to the requirements for FeB 400 HN NR* (see figure A2).

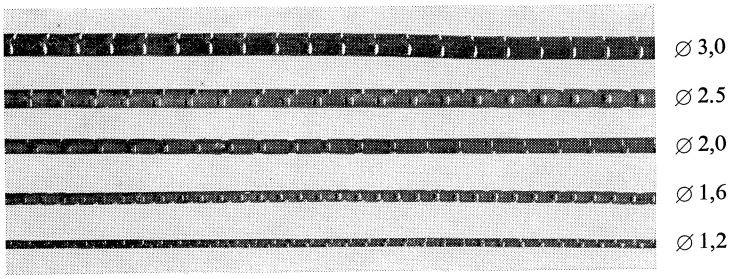

Fig. A2. Model reinforcing bars (actual size).

To check the quality of the steel its yield point, tensile strength and elongation at fracture were determined. The results were as follows:

$f_e = 425$ N/mm^2 and $f_{ar} = 520$ N/mm^2 (series I, II, III, IV);
$f_e = 450$ N/mm^2 and $f_{ar} = 550$ N/mm^2 (series V).

These are average values of approximately ten test-pieces per bar diameter; the maximum deviation was approximately 2%. The elongation at fracture, measured on a length equal to five times the diameter, was above 25%. The average stress-strain diagram for all the bars is presented in figure A3; a gauge length of 200 mm was adopted as the standard of comparison for the strain.

In all the test specimens the bending moment reinforcement was installed in the form of an orthogonal mesh (the bars were interconnected at only a limited number of their intersections). What punching shear reinforcement was additionally provided in the specimens of series II is indicated in figure A1.

* The originally plain bars were provided with indentations by IBBC-TNO to give them bond properties comparable to those of ribbed reinforcing bars. This steel is successfully emloyed in many model tests.

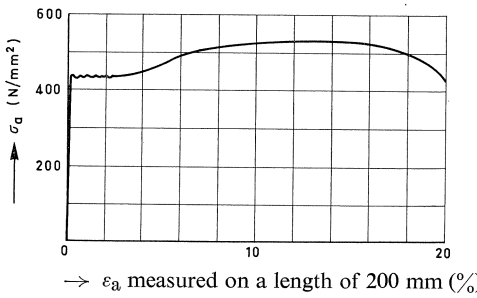

Fig. A3. Average stress-strain diagram of the model bars.

The columns were also reinforced. In series I to IV the main reinforcement in each column comprised eight 2,5 mm bars (except for the specimens I-3 and I-4, in which twelve 3 mm and four 2,5 mm bars were provided respectively). The stirrups consisted of 1,2 mm bars. The column reinforcement in series V comprised twenty-two 3 mm bars (or twenty-five 3 mm bars for the specimens V-3′ and V-6′), with 1,6 mm stirrups.

The reinforcement used in a number of the specimens is illustrated in figure A4.

4 Composition of the concrete

The composition of the micro-concrete was as follows:

aggregate/cement ratio 4,63
water/cement ratio 0,45
cement: portland cement, class B (Encilite)
fineness modulus 3,91
grading:

on sieve	cumulative residue (%)
d–2,8	50
d–1,4	70
d–0,60	80
d–0,300	92
d–0,150	99
0	100

For the purpose of determining the quality (strength class) of the concrete, 40 mm test cubes were also cast. These were tested by crushing them with the interposition of 0,5 mm thick cardboard. The cube (compressive) strengths obtained on the day on which the tests were performed on the column-and-slab specimens are listed in table A1.

The test specimens and the corresponding cubes were stored indoors at a temperature of about 20° C and relative humidity of 50% (on average). The formwork was removed from the slab three days after concreting.

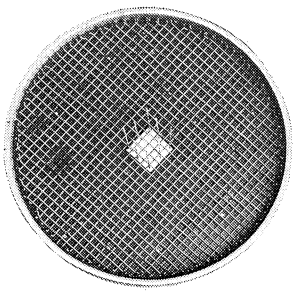

specimen II-7

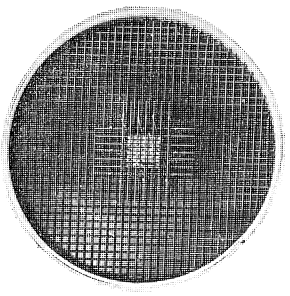

specimen II-8

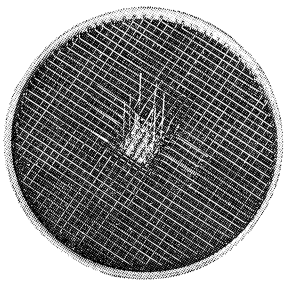

specimen II-9

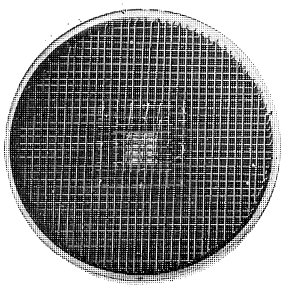

specimen II-10

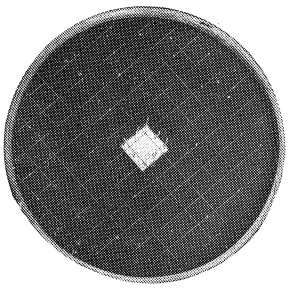

specimen III-12

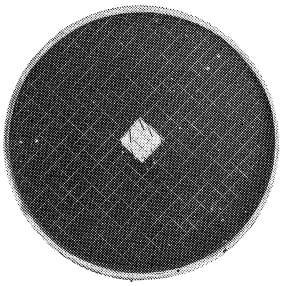

specimen III-13

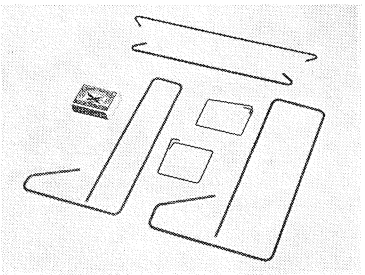

shapes of reinforcing bars

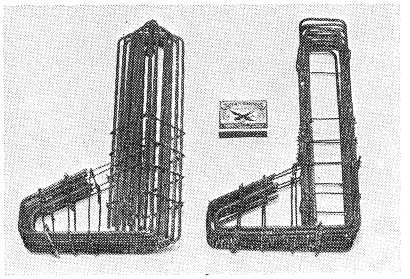

reinforcement cages for the columns of the specimens in series V

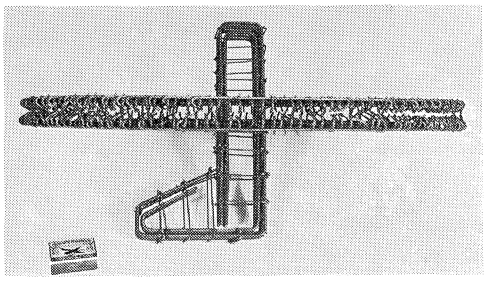

specimen V-2′

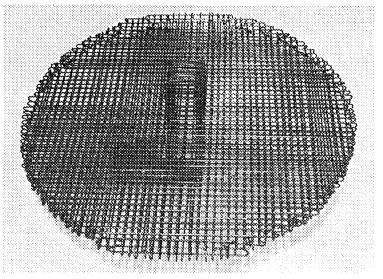

specimen V-2′

Fig. A4. Reinforcement provided in a number of specimens.

5 Execution of the tests; program of measurements

The test set-up is shown schematically in figure A5 and is also illustrated in figure A6. The axially loaded specimens were supported at the perimeter on a closed steel ring at a distance of 25 mm from the edge of the slab. A load-distributing layer of cardboard, 3 mm thick, was interposed between this ring and the slab. The eccentrically loaded specimens were additionally provided with an identical ring on the other side of the slab.

The load was applied to the column through the ball of a load cell, a steel plate and a 3 mm thick cardboard load-distributing layer. The load was raised by means of a pump and jack and was measured by means of the load cell and associated measuring apparatus.

In order to facilitate observation of cracking, the slab was tested with its bending moment reinforcement upwards. The column was therefore thrust upwards by the load applied. Dial gauges for determining the deflection were mounted on the top of the test specimen.

6 Cracking

6.1 *Axially loaded specimens*

The cracking that occurred in four of the test specimens in various stages of loading is illustrated in figure A7. The other specimens in the series I to IV showed similar crack patterns.

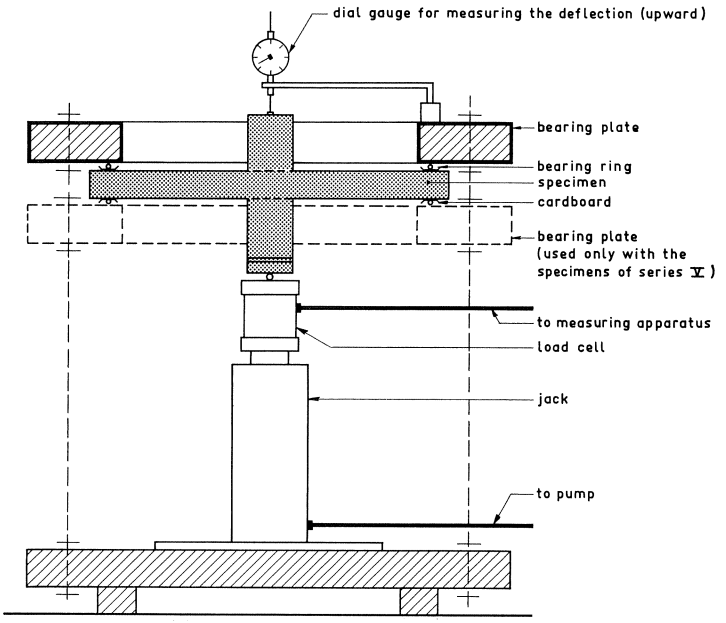

Fig. A5. Diagram of test set-up (the force is applied in the upward direction).

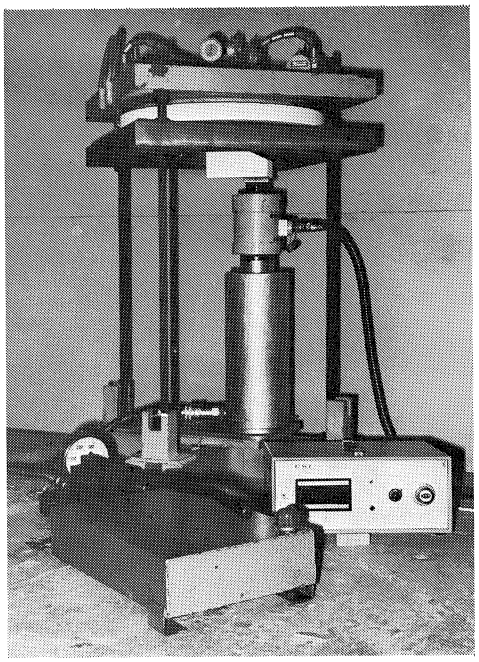

Fig. A6. Set-up for testing the eccentrically loaded specimens.

With increasing load, radial cracks first appeared on the tension side of the slab. The entirely unreinforced slab (specimen III-11) failed almost simultaneously with the formation of these cracks. The load that this slab was nevertheless able to carry is attributable to the strength of the concrete, a factor which normally is entirely neglected in the calculation of the theoretical failure moment. A very lightly reinforced slab fails as a result of yielding of the reinforcing steel at the radial cracks. For example, in figure A7: specimen III-13 with $\omega_0 = 0{,}2\%$.

In a slab with a somewhat higher percentage of reinforcement (specimen III-15 with $\omega_0 = 0{,}6\%$) the formation of radial cracks is followed by tangential cracking in the vicinity of the column. In the stage of failure the radial cracks open wide in consequence of yielding of the reinforcement. Finally, without any appreciable further increase of the load, a conical piece is punched through the slab as a result of the inclined tangential cracks already present and of the stresses in the remaining compression zone of the concrete.

The behaviour of the specimens III-13 and III-15 is determined by bending moment failure as the failure criterion.

In the case of more heavily reinforced specimens (e.g., specimen IV-17 with $\omega_0 = 1{,}3\%$) the radial cracks are relatively short and narrow, while their formation is almost simultaneously accompanied by the visible emergence of tangential cracks as well. Failure occurs along a conical crack, while the other cracks do not open wide. With an even higher percentage of reinforcement (test specimen IV-19 with $\omega_0 = 2{,}1\%$)

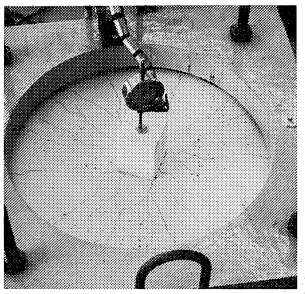

$F = 7$ kN

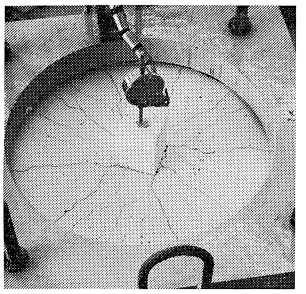

$F = 8$ kN

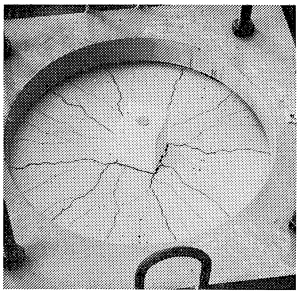

at $F_{max} = 8{,}9$ kN
failed in bending moment

specimen III-13, $\omega_0 = 0{,}2\%$

$F = 10$ kN

$F = 14$ kN

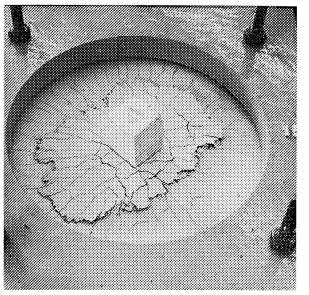

at $F_{max} = 21{,}1$ kN
failed in bending moment

specimen III-15, $\omega_0 = 0{,}6\%$

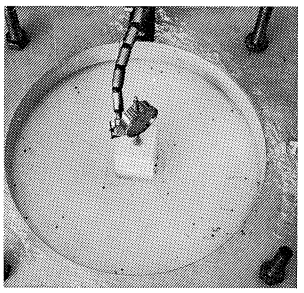

$F = 12$ kN

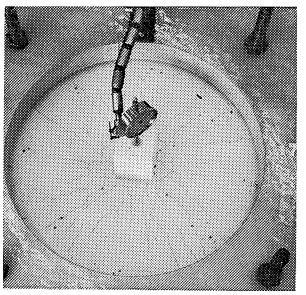

$F = 20$ kN

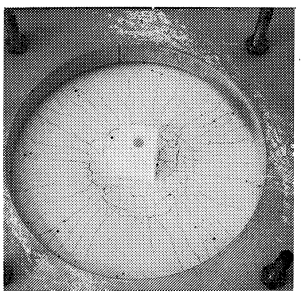

at $F_{max} = 26$ kN
failed in punching shear

specimen IV-17, $\omega_0 = 1{,}3\%$

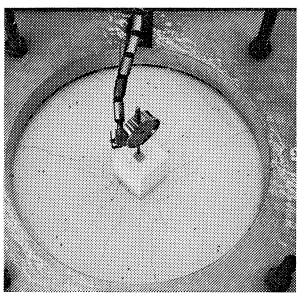

$F = 20$ kN

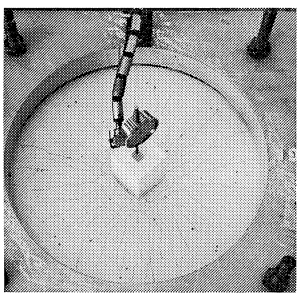

$F = 28$ kN

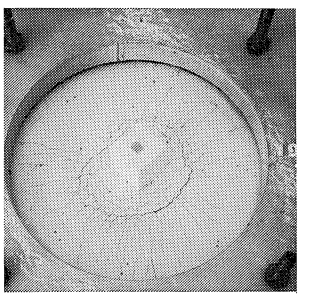

at $F_{max} = 30$ kN
failed in punching shear

specimen IV-19, $\omega_0 = 2{,}1\%$

Fig. A7. Crack patterns and failure patterns of some specimens.

the radial cracks are even less pronounced. The specimen fails along the conical tangential cracks which had first developed simultaneously with the radial cracks. The behaviour of the specimens IV-17 and IV-19 therefore indicates punching shear as the failure criterion; the radial cracks do not open wide, because at failure the reinforcement is not stressed up to the yield point of the steel.

The specimens II-8 and II-10, which contained punching shear reinforcement, behaved in approximately the same manner as the specimens without punching shear reinforcement but with an equal percentage of bending moment reinforcement. The conical shape begins on the compression side of the slab always directly at the column, in accordance with figure 6. An exception is formed by specimen II-9 with inclined punching shear reinforcement. In that case the tangential cracks are dispersed somewhat farther from the column (see figure A8) and the conical surface of fracture

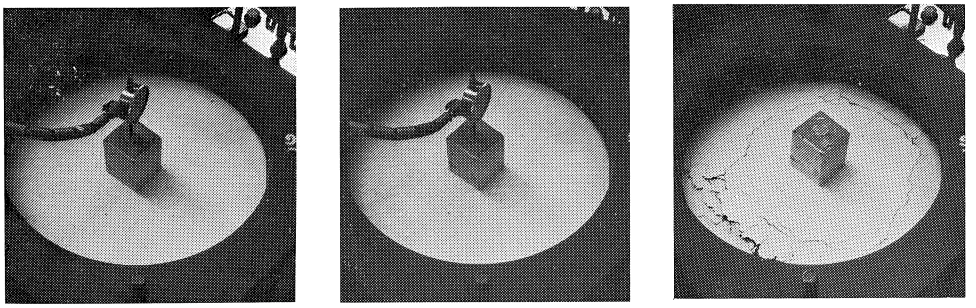

$F = 20$ kN | $F = 28$ kN | at $F_{max} = 40$ kN failed in punching shear

Fig. A8. Crack patterns and failure pattern of specimen II-9 (with inclined punching shear reinforcement).

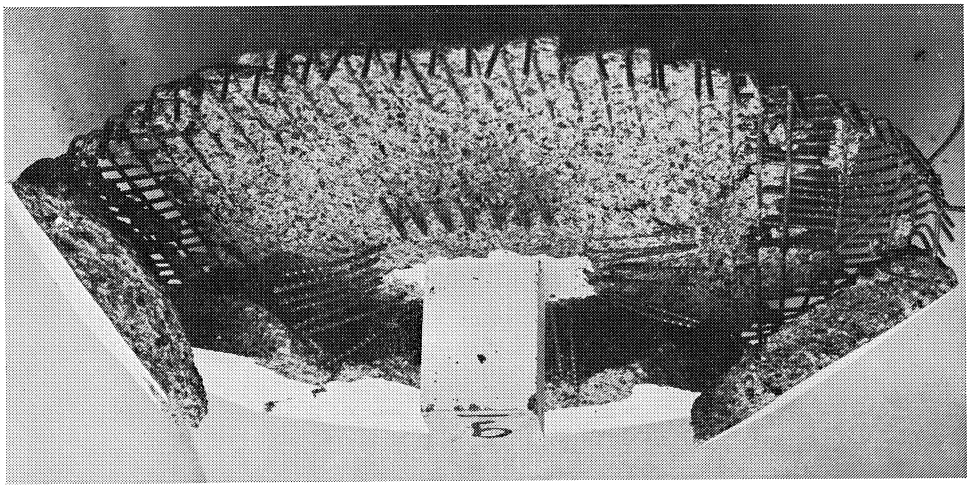

Fig. A9. Underside of specimen II-9 (with inclined punching shear reinforcement) after loading to failure.

begins, on the compression side of the slab, at some distance from the column. As appears from figure A9, the fracture surface extends approximately through the point of bending of the inclined reinforcement.

6.2 *Eccentrically loaded specimens*

In the main, the cracking of the eccentrically loaded specimens (series V) corresponds to that of the axially loaded ones. As a result of the eccentricity of the load, however, a crack pattern is formed which is intermediate between that for axial loading and that for a pure bending moment (see figure 10).

For practically all the eccentrically loaded specimens it is indeed found that the region located diametrically opposite the line of action of the load displays little or no cracking. Failure likewise occurs along a conical surface, but the conical shape is somewhat less distinctly developed, while there is a noticeable "displacement" of the cone towards the load. The following cases will be considered by way of illustration.

In the specimens V-23′ and V-24′ with $\omega_0 = 0{,}3\%$ and a relatively large eccentricity ($e/a = 1{,}125$ and 1,500 respectively) radial cracks spread out only from the side of the

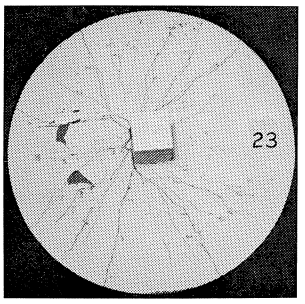

specimen V-23′
$\omega_0 = 0{,}3\%$

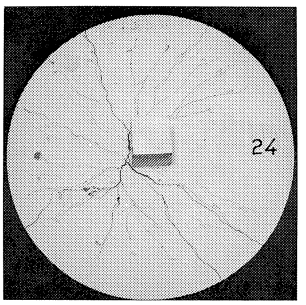

specimen V-24′
$\omega_0 = 0{,}3\%$

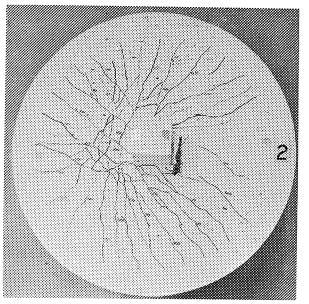

specimen V-2′
$\omega_0 = 1{,}8\%$

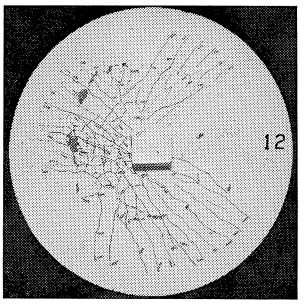

specimen V-12′
$\omega_0 = 1{,}2\%$

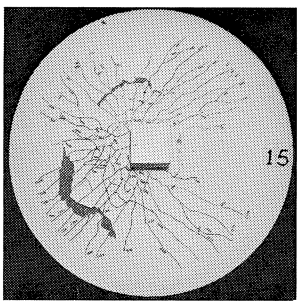

specimen V-15′
$\omega_0 = 1{,}5\%$

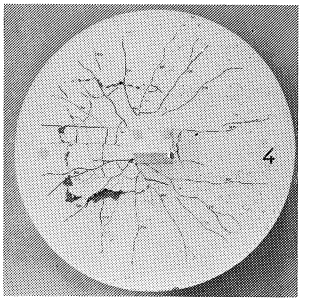

specimen V-4′
$\omega_0 = 0{,}6\%$

Fig. A10. Some failure patterns of eccentrically loaded specimens; the load was applied at the left of the axis of the column.

column adjacent to the load (see figure A10). In this stage there occurred yielding of the reinforcement, so that failure was due to bending moment.

The specimens V-2′, V-3′, V-12′ and V-15′ with $\omega_0 = 1{,}2$ to $1{,}8\%$ and $e/a = 1{,}5$ at first developed radial cracks and then showed heavy tangential cracking, in the course of which the conical shape again clearly manifested itself (see figure A10). Incidentally, these specimens failed in punching shear at a much lower load than could be expected on the basis of the theoretical considerations on bending moment failure (see 3.4).

With reference to the specimens V-2′ and V-3′ it should furthermore be mentioned that a compression zone developed at the top of the slab, and some slight degree of crushing of the concrete occurred there (see figure A10, to the right of the column). Yet no cracking on the underside of the slab occurred in any of the specimens concerned.

Specimen V-4′ with $\omega_0 = 0{,}6\%$ and $e/a = 1{,}5$ is a borderline case. In this case the theoretical failure loads F_{ut} and F_{ub} differ little from each other (see, for example, also figure 14). The failure pattern according to figure A10 does indeed display a mixed form of the crack patterns referred to above.

7 Deflection and angular rotation

In figures A11 to A16 the deflection of the slab at the column in relation to the bearing has been plotted against the corresponding load. For the eccentrically loaded specimens of series V this deflection has been taken as the average of the values measured at the edges of the column. For this last-mentioned series the angular rotation φ of the axis of the column in relation to the plane through the bearings is also indicated.

Understandably, the deflection measurements reveal the same behaviour as is manifested also by the cracking of the specimens. The entirely unreinforced slab (specimen III-11, figure A13) fails almost immediately after the formation of a small number of radial cracks, as a result of which the deflection more or less suddenly increases indefinitely. The slabs in which yielding of the reinforcement is the determinative phenomenon undergo a relatively large deflection before the maximum load is reached (specimens I-5, III-11, 12, 13, 14, 15, (16) and V-(4′), 17′, 18′, 19′, 20′, 21′, 22′, 23′, 24′). On the other hand, in the specimens with a high percentage of reinforcement the deflection prior to failure is relatively small and is smaller according as the reinforcement percentage is higher. The specimens provided with punching reinforcement (specimens II-8, 9 and 10) undergo virtually the same deflections as the corresponding specimens without punching shear reinforcement but with identical bending moment reinforcement (see figure A12).

With greater eccentricity of the column load the deflection is found to increase also. This is true of the specimens for which punching shear (e.g., V-1′, 7′, 8′, 9′ and 2′) and of those for which bending moment (e.g., V-20′, 21′, 22′, 23′ and 24′) was the cause of failure.

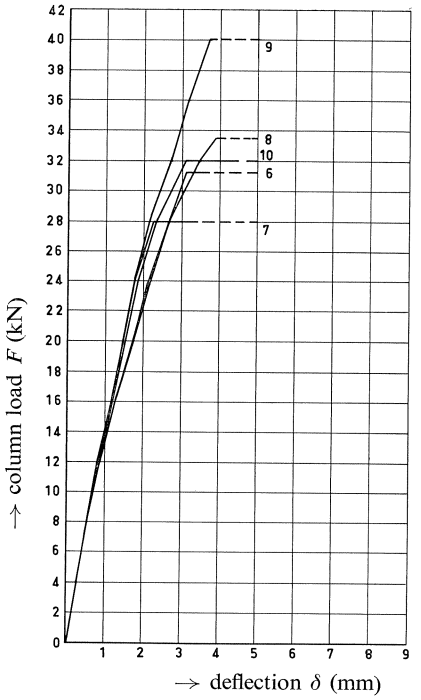

Fig. A11. Deflection of specimens of series I.

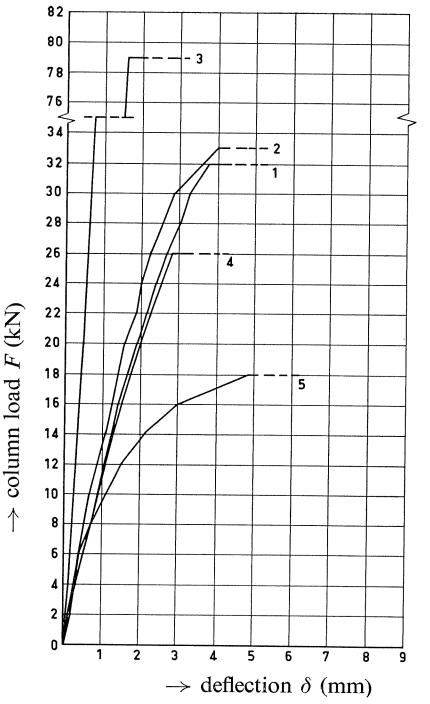

Fig. A12. Deflection of specimens of series II.

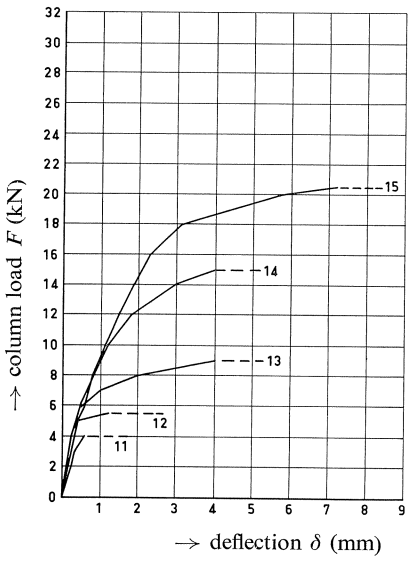

Fig. A13. Deflection of specimens of series III.

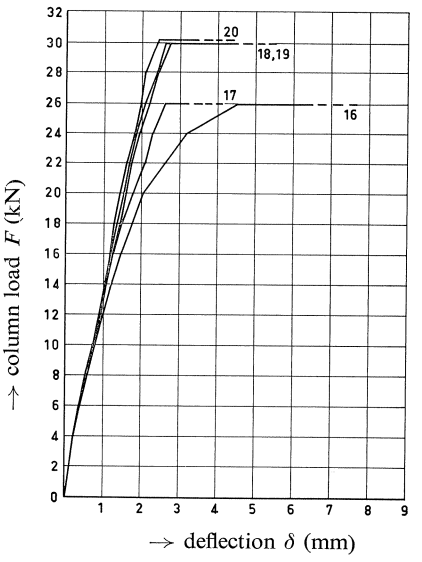

Fig. A14. Deflection of specimens of series IV.

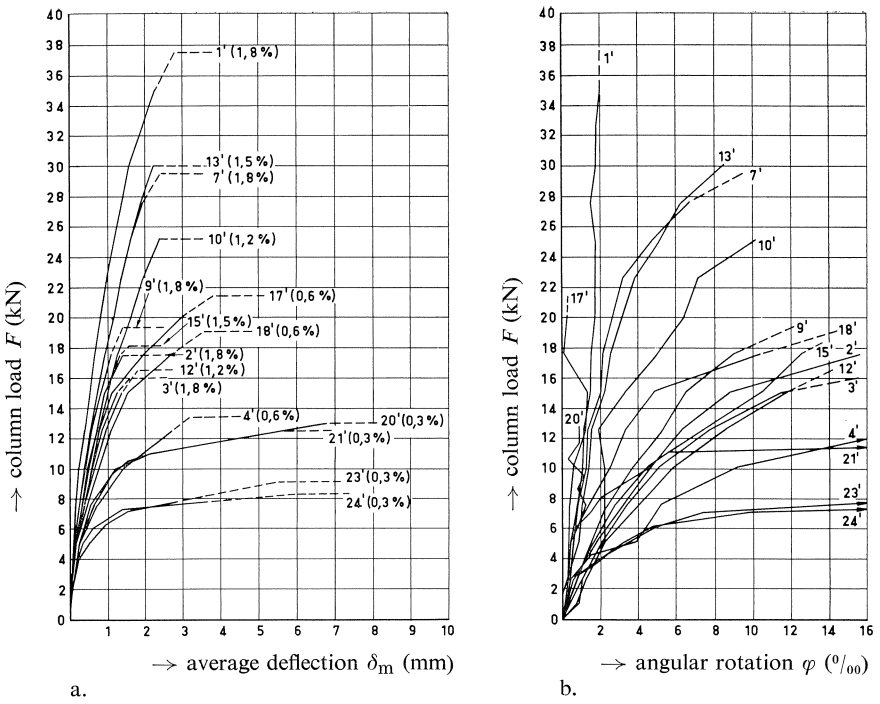

Fig. A15. Average deflection and angular rotation of the statically loaded specimens of series V.

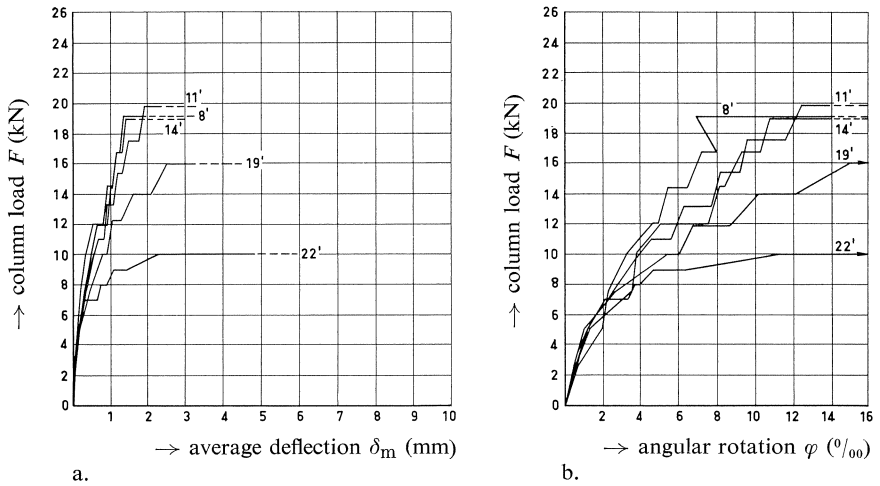

Fig. A16. Average deflection and angular rotation of the alternatingly loaded specimens of series V.

8 Failure load

The magnitude of the failure load (the maximum force on the column that a specimen was able to resist) is given in Table A1. On attainment of this maximum there was a partial falling-off in the magnitude of the load because the deformation rather suddenly increased indefinitely. It was not possible to restore the load to the value it had reached before. The large deformation produces the pattern illustrated in figures A7 and A8 (right-hand photographs), this being associated with the formation of radial cracks also on the underside of the slab. The photographs presented in figures 6 and A9 were taken after the specimen in question had subsequently been broken up by further loading (at a value less than F_{max}).

Up to a reinforcement percentage of about 0,9% the bending moment reinforcement is found to affect the magnitude of the axial failure load. A further increase in the percentage does not appreciably increase the load capacity of the specimen, because then failure in shear (i.e., punching shear) becomes the determining factor. For $\omega_0 > 0{,}9\%$ the deviant failure load behaviour is attributable to a difference in the concrete quality, the column thickness, the slab thickness (no. I-3) and the normal scatter.

In principle, the same applies to eccentric load on the column, except that the limit value of ω_0 will decrease according as the eccentricity e is larger. This is most clearly evident from figure 14.

With regard to punching shear reinforcement it is to be remarked that in the specimens II-8 and II-10, containing one and two layers of such extra reinforcement respectively, it did not produce any noticeably more favourable result. In the case of specimen II-9 with inclined reinforcement, however, there was an improvement. The inclined reinforcement was evidently able to increase the strength of the otherwise determinative conical section to such an extent that a conical fracture surface of larger diameter became the determinative one, the larger area of this surface being of course associated with a higher failure load.

9 Alternating load

In the case of the specimens V-8′, 11′, 14′, 19′ and 22′, at four or five different values of the applied load, the magnitude of the load was varied between that level and a minimum load of approximately 0,4 kN, at a frequency of 1 cycle/sec. At each load level the alternations were stopped when it was found that the deformation of the specimen had ceased to undergo any appreciable further increase (mostly after about 1000 alternations) or when the specimen had failed after undergoing a very great increase in deformation. The specimens V-8′ and 14′, which can be assumed to have failed in punching shear, are found to have attained an approximately 17% lower failure load than might have been expected on the basis of interpolation of the failure loads of comparable specimens subjected to static load (for example, see figures 13 and 14).

Nevertheless it appears that for these two specimens the value of $\zeta = F_{max}/\alpha_t F_{ut}$ is amply in excess of 1. The other specimens subjected to load alternations do not display any deviant behaviour.

APPENDIX B

References

[1] CEB Bulletin d'Information No. 57. Dalles, structures planes. Thème II: Poinçonnement (Slabs, plane structures. Theme II: Punching shear). September 1966.

[2] MAST, P. E., Stresses in flat plates near columns. Journal of the American Concrete Institute, October 1970.

[3] HANSON, N. W. and J. M. HANSON, Shear and moment transfer between concrete slabs and columns. Journal of the Portland Cement Association, January 1968.

[4] MOE, J., Shearing strength of reinforced concrete slabs and footings under concentrated loads. Bulletin D 47 of the Portland Cement Association, April 1961.

[5] Praktische richtlijnen CEB. Dutch translation of the original French edition of the CEB Recommendations: Recommandations pratiques unifiées pour le calcul et l'exécution des ouvrages en béton armé. Publ. Betonvereniging, May 1966.

[6] CEB Bulletin d'Information No. 84: Recommandations internationales CEB-FIP-1970 pour le calcul et l'exécution des ouvrages en béton (CEB-FIP 1970 international recommendations for the design and construction of concrete structures), May 1972.